The energy master equation

a low-temperature approximation to Bässler's random walk model

Dyre, Jeppe

Publication date:
1994

Document Version
Også kaldet Forlagets PDF

Citation for published version (APA):
Dyre, J. (1994). *The energy master equation: a low-temperature approximation to Bässler's random walk model*. Roskilde Universitet. Tekster fra IMFUFA Nr. 286 http://milne.ruc.dk/ImfufaTekster/

TEKST NR 286 1994

The energy master equation: A low-temperature approximation to Bässler's random walk model

By: Jeppe C. Dyre

TEKSTER fra

IMFUFA ROSKILDE UNIVERSITETSCENTER
INSTITUT FOR STUDIET AF MATEMATIK OG FYSIK SAMT DERES FUNKTIONER I UNDERVISNING, FORSKNING OG ANVENDELSER

IMFUFA, Roskilde Universitetscenter, Postboks 260, 4000 Roskilde

The energy master equation: A low-temperature approximation to Bässler's random walk model

by: Jeppe C. Dyre

IMFUFA tekst nr. 286/94 80 pages ISSN 0106-6242

ABSTRACT

The first part of this paper deals with the justification of Bässler's phenomenological "random walk model" for viscous liquids [H. Bässler, Phys. Rev. Lett. **58**, 767 (1987)], which considers the random walk of a particle (representing the liquid state) on a d-dimensional infinite cubic lattice with site energies randomly chosen according to a Gaussian. The random walk model is derived from Newton's laws by making a number of simplifying assumptions. Thus, the significance of the model is emphasized as a "canonical" phenomenological model for relaxations in viscous liquids and at the glass transition. In the second part of the paper an approximate low-temperature description of energy fluctuations in the random walk model - "the energy master equation" (EME) - is arrived at. The EME is derived by arguing that percolation dominates the relaxational properties of the random walk model at low temperatures. The approximate EME description of the random walk model is expected to be valid at low temperatures at long times in high dimensions. However, computer simulations show that the EME works well already in two dimensions. The EME is one-dimensional and involves only energy; it has no randomness and is completely specified from the density of states, the attempt frequency, and the percolation energy of the random walk model. The EME allows a calculation of the energy probability distribution for an arbitrarily varying temperature as function of time at realistic laboratory time scales; it is probably the only model with this property that is also explicitly consistent with statistical mechanics. The final part of the paper gives a comprehensive discussion, comparing the EME to related work and listing the EME's qualitatively correct predictions, its new predictions, and some "wrong" predictions, most of which goes against the most common pictures of viscous liquids and the glass transition without necessarily violating experiments.

1. INTRODUCTION

The glass transition takes place when a liquid upon cooling becomes more and more viscous and finally solidifies to form a glassy solid [1-14]. Most, or perhaps all, liquids are able to form glasses when cooled sufficiently fast to avoid crystallization. Examples of glasses include the classical oxide glasses [15], ionic glasses [16], polymers [6,17,18], metallic glasses [19], and glasses made by cooling organic liquids to low temperatures [20,21]. Even simple liquids form glasses in computer experiments, where extremely high cooling rates are possible [12,22,23]. Spin glasses are examples of non-liquid systems that exhibit glassy features [24,25].

The glass transition is still far from well-understood, but the kinetic nature of the transition is not in doubt. Thus, the glass transition is not a phase transition, though it is thermodynamically similar to a second order phase transition. This is evidenced by several facts universally observed: The transition is not sharp, the glass transition temperature depends on the cooling rate, and the transition is irreversible and exhibits various hysteresis phenomena. The dynamic nature of the glass transition complicates the problem considerably.

Viscous liquids close to the glass transition have common features, a broad distribution of relaxation times and a stronger than Arrhenius temperature-dependence of the viscosity. Close to the glass transition there are further common characteristics like the overshoot (hysteresis) of the specific heat upon reheating [8,14], the cross-over effect [8] or the prepeak upon

the melting of a well-annealed glass [11]. The universal character of viscous liquids and the glass transition motivates a search for a phenomenological model valid for any viscous liquid.

While phenomenological models of viscous liquids and the glass transition have been studied for many years, the 1980's brought a new theory, the mode-coupling theory [26,27]. In a number of well-defined steps this theory traces the viscous behavior and the glass transition back to Newton's laws for the [classical] motion of the molecules. Extensive work has gone into studying the mode-coupling theory and comparing it to experiment. At present there seems to be a growing consensus [28] that mode-coupling theory gives an accurate description of the onset of viscous behavior, when the relaxation times are shorter than about 1 nanosecond. However, the theory is not able to explain the more viscous regime and the laboratory glass transition. This is because the activated "hopping" type processes that dominate this regime are not accounted for [28-30]. Thus, the focus is now once again on attempts to formulate a phenomenological model that captures the essentials of viscous liquids and the glass transition.

Since the glass transition is a kinetic "freezing" of the viscous liquid, a phenomenological model should first of all mimic the basic physics of viscous liquids in thermal equilibrium. An important characteristic here is the **average relaxation time** of the viscous liquid, τ, which is a direct measure of the time needed for molecular rearrangements. The average relaxation time may be determined, e. g., as the inverse

dielectric, mechanical or specific heat loss peak frequency. Alternatively, it may be calculated from the viscosity, η, and the infinite frequency shear modulus, G_∞, by means of the expression

$$\tau = \frac{\eta}{G_\infty} \quad . \tag{1}$$

These definitions do not give exactly identical τ's [13], but the difference is insignificant for the present discussion. Typical values of τ for glass forming liquids lie in the millisecond, second or even hour range. These times are to be compared to the average vibration time, which is of order one picosecond.

The basic thing one would like to understand about the average relaxation time is its non-Arrhenius temperature dependence; for almost all viscous liquids τ has an apparent activation energy that increases as the temperature decreases. Since models assuming some distribution of energy barriers usually lead to the opposite behavior, explaining $\tau(T)$ is a real challenge, but also a likely key to understanding viscous liquids.

The phenomenological models may be roughly classified into two types (an alternative to the below classification has been given by Scherer in an excellent review of relaxation in viscous liquids [29]). One type of models, "type I", are models that have a non-Arrhenius $\tau(T)$, but otherwise do not attempt to model the liquid. These models are so simple that they can be analyzed in detail [31]. Examples of "type I" models are Derrida's random

energy model [32], the kinetic Ising model [33], or the tiling model of Stillinger and coworkers [34]. The other type of model, "type II", attempt to model the physics of real viscous liquids. In all "type II" models the liquid is assumed to be divided into "cooperatively rearranging regions". The "type II" models can be further classified according to which thermodynamical quantity controls τ, **entropy**, **volume**, or **energy**.

A well-known entropy-controlled model is the theory of Gibbs and coworkers [35,36]. This model correlates the non-Arrhenius behavior with the Kauzmann paradox [2,11], the fact that the configurational entropy extrapolates to zero at a finite temperature, T_K: The model predicts that the average relaxation time follows the Vogel-Fulcher-Tammann (VFT) law [11,29], where A is a constant and the characteristic temperature T_o is predicted to be equal to T_K,

$$\tau = \tau_o \, e^{\frac{A}{T-T_o}} \quad . \tag{2}$$

The Vogel-Fulcher law gives a good fit to $\tau(T)$ for many viscous liquids and one also finds that T_o in most cases is indeed close to T_K [11].

The entropy model predicts that underlying the glass transition there is a genuine second order phase transition at $T=T_o>0$ to a state of zero configurational entropy. Still, there are a number of problems with this approach. The original Gibbs-DiMarzio model [35] was based on a mean-field theory for polymers

that later was shown to be incorrect [37], and the Adams-Gibbs [36] derivation of Eq. (2) is hard to understand in detail. Furthermore, the Vogel-Fulcher law seldomly applies in the whole temperature range of interest; usually deviations occur close to the glass transition where the average relaxation time is less temperature dependent than predicted [8,20,29]. Finally, it should be noted that the Kauzmann paradox does not have to be a paradox. As shown by Angell and Rao many years ago [38], even a system with only two energy levels has an entropy which, if only known at high temperatures, extrapolates to zero at a positive temperature. Though this model does not fit experiment, the excess entropy data may be fitted with a model with only a finite number of energy levels and thus a positive entropy at any positive temperature [39].

The standard example of a volume-controlled model is the "free volume model" [40]. In this model, the average relaxation time is determined by the volume freely available for cooperative rearrangements of the molecules, V_f, according to the expression $\tau \propto \exp(C/V_f)$. In the simplest version of the model the free volume decreases linearly with decreasing temperature, leading to a non-Arrhenius $\tau(T)$ of the VFT-type (Eq. (2)).

In energy-controlled models one formulates a master equation [41] governing the dynamics of the cooperatively rearranging regions. The relevance of energy [i. e., potential energy] was emphasized already in 1969 by Goldstein [42]. More recently, Brawer proposed a model where transitions between different states occur via excitations to a common high lying

energy level [8,43]. This picture is based on ideas that go back to Goldstein [39]. Brawer's model was later simplified [44] to a one-dimensional model where the only relevant parameter is the energy.

Bässler's "random-walk model" [45,46] is an energy-controlled model, which is similar to those used in the description of AC conduction in disordered solids [47,48] and of energetic relaxation and diffusion of electronic excitations in random organic solids [49]. This model, which is the subject of the present paper, considers the random walk of a "particle" on a cubic lattice in d dimensions, where each site has an energy randomly chosen according to a Gaussian. The "particle" represents the state of a cooperatively rearranging region. For the random walk model $\tau(T)$ is given [45,46] by

$$\tau = \tau_o \exp\left(\frac{A}{T^2}\right) \quad . \tag{3}$$

This simple expression fits experiment surprisingly well [45,46,50,51]. An even better fit is obtained by using the following generalization of Eq. (3): $\tau=\tau_o\exp(A/T^n)$ [20,21,52].

In a recent paper by Arkhipov and Bässler [53] the random walk model was extended into a model that reduces to the original model at high temperatures - the "real liquid" regime - while at low temperatures - the "supercooled melt" regime - the system is described by the energy master equation. The idea [53] is that, at high temperatures direct jumps between metastable states are possible because the energy landscape itself fluctuates; these jumps correspond to an elementary step on the d-dimensional

lattice of the original random walk model. At low temperatures, on the other hand, the landscape fluctuations are frozen on the relevant time-scale and each jump leads to a totally new configuration, the dynamics here being described by the energy master equation.

The purpose of the present paper is to show that the energy master equation, assumed by Arkhipov and Bässler to describe the different physics going on at low temperatures, in fact gives a good description of the low-temperature behavior of the **original** random-walk model. Thus, in a sense the Arkhipov-Bässler model is contained in Bässler´s original and simpler random-walk model. The low-temperature approximate description via the energy master equation contains no adjustable parameters. This approximation is arrived at by arguing that **percolation** in the random-walk model becomes important at low temperatures. The "transition state energy" of the energy master equation is identified with the highest energy met on a percolation path. In effect, one arrives at a picture which is close to that recently proposed by Hunt [13,54], where the low-temperature properties of viscous liquids are dominated by percolation.

The paper has the following outline. In Sec. 2 a justification of the random walk model is sketched, where the model is traced back to Newton's laws for the molecules of a cooperatively rearranging region. This section supplements the original arguments for the model given by Bässler [45,46]. In Sec. 3 the approximate energy master equation is derived. In Sec. 4 computer simulations are presented comparing the random walk model and the energy master equation. Section 5 discusses

what to expect at the glass transition according to the energy master equation. Section 6 gives a comprehensive discussion which includes a qualitative comparison to experiment. Finally, Sec. 7 gives the conclusions.

2. THE RANDOM WALK MODEL AND ITS "DERIVATION" FROM NEWTON'S SECOND LAW.

The purpose of this section is to "derive" the random walk model [45,46] from the equations of motion for the molecules of the viscous liquid. The "derivation", which proceeds in five steps, is not rigorous, but rather an attempt to make explicit the assumptions that needs to be made in order to justify the model from basic principles. The "derivation" indicates that the random walk model could be regarded as **the** canonical phenomenological model for viscous liquids and the glass transition. The viewpoints presented below are similar to those of Bässler, but there are also some differences as will be discussed at the end of this section.

Before presenting the "derivation" of the random walk model we recall the exact definition of the model. The model considers the random walk of a "particle" in d dimensions on an infinite cubic lattice. The "particle" represents the state of the region, which is thus completely specified by d integer coordinates. Each state has an energy, E, which is chosen

randomly according to a Gaussian with variance σ:

$$n(E) = \frac{1}{\sqrt{2\pi\sigma^2}} \exp\left(-\frac{E^2}{2\sigma^2}\right) \quad . \tag{4}$$

The energies of adjacent states are uncorrelated. The dynamics of the system is described by a master equation [41], specifying the time development of the probability that the "particle" is in state i, P_i. If $\Gamma(i \to j)$ is the transition rate for jumps from state i to state j, the general master equation [41] is

$$\frac{dP_i}{dt} = -\sum_j \Gamma(i \to j) P_i + \sum_j \Gamma(j \to i) P_j \quad . \tag{5}$$

The first term describes "particles" jumping away from state i and the second term describes "particles" jumping into state i. In random walk models the transition rates are usually chosen to be zero except for nearest neighbor jumps (i. e., where a single coordinate changes plus or minus one). If $\beta = 1/(k_B T)$ and Γ_o is the attempt frequency, the transition rate for nearest neighbor jumps is in Bässler's random walk model given by Metropolis dynamics,

$$\Gamma(i \to j) = \begin{cases} \Gamma_o & , \quad E_i > E_j \\ \Gamma_o e^{-\beta(E_j - E_i)} & , \quad E_i < E_j \end{cases} \tag{6}$$

It is physically realistic to assume that Γ_o is of order 10^{12} Hz, corresponding to a typical phonon frequency.

What kind of predictions can be made from the random walk model? The model predicts how the average energy changes in time

for any externally controlled time-dependent temperature. This includes monitoring how the energy relaxes to equilibrium from a non-equilibrium state, or how the dynamic specific heat changes through the glass transition. In particular, the average relaxation time for energy relaxations close to equilibrium can be calculated as a function of temperature. Also, the equilibrium frequency-dependent specific heat may be obtained.

We now proceed to justify the random walk model from basic principles in five steps, assuming the molecules of the viscous liquid are described by classical mechanics.

Step 1: The Region Assumption. All type II models for the dynamics of viscous liquids assume cooperative "flow events" that are localized to small "regions" of the liquid [6,8,36,39,42,55-60]. These regions have been called "cooperatively rearranging subsystems" [29] or " - regions" [36] , "quasi-independent units" [39], "thermokinetic structures" [58], "molecular domains" [59], or "dynamically correlated domains" [60]. The picture of viscous flow, proceeding via strongly cooperative motion of particles confined to small regions of the liquid, has been confirmed by computer simulations [61,62]. The "region assumption", however, is not just the quite reasonable idea that flow events are strongly localized. The assumption is the much stronger one that the liquid may be regarded as an ensemble of non-interacting regions. There are two potential problems with the region assumptions. It ignores region-region interactions which may be important because the regions are expected to be relatively small (some 10-20 Å [58]). Also, the picture is static and not easy to relate to an actual flow that will deform the regions.

Nevertheless, the region assumption is necessary to arrive at a simple phenomenological model.

Step 2: Replacing Newton's laws with Langevin dynamics. From now on the attention is confined to a single region, the molecules of which move according to Newton's laws. The motion is deterministically determined by the potential energy as function of the molecular coordinates, $U(Q_1,..,Q_d)$. The importance of the potential energy "surface" for understanding viscous liquids and the glass transition has been emphasized in a number of papers [11,30,39,42,63,64]. Following the tradition in polymer physics [65], we now replace Newton's equations of motion by stochastic Langevin equations (similar non-deterministic equations are used for the description of Brownian particles suspended in liquids [66]). The Langevin equations of motion [41,65] are

$$\dot{Q}_i = -\mu \frac{\partial U}{\partial Q_i} + \xi_i(t) \quad (i=1,..,d) \quad , \tag{7}$$

where $\xi_i(t)$ is a Gaussian stochastic white noise term:

$$\langle \xi_i(t)\, \xi_j(t') \rangle = 2\mu k_B T\, \delta_{i,j}\, \delta(t-t') \quad . \tag{8}$$

The crucial property of the Langevin equations of motion is [41,65] that each state is visited with the correct "canonical" probability of statistical mechanics,

$$P_o(Q_1,..,Q_d) = Const.\ \exp[-\beta U(Q_1,..,Q_d)] \tag{9}$$

Physically, the assumption of Langevin dynamics is reasonable for viscous liquids [67], because the molecules collectively vibrate

in potential energy minima for long times before occasionally "jumping" to another potential energy minimum. And the rate of jumps between two energy minima is, for both Newtonian and Langevin dynamics dominated by a factor $\propto \exp(-\beta \Delta U)$ [68], where ΔU is the energy barrier to be overcome.

Step 3: From Langevin dynamics to a hopping model. We now proceed to discretize the spatial variables of the Langevin equations. The resulting state space is a d-dimensional cubic lattice. It is reasonable to assume that, since the underlying Langevin dynamics has a continuous trajectory, only nearest neighbor jumps are allowed on the lattice. For the jump rates those given by Eq. (6) are an obvious choice: Unless infinitely steep potentials are allowed, the Langevin equation implies that it takes some definite time to travel the discretization length downhill; in the discrete version this means there should be a maximum jump rate. If, the discretization is to be self-consistent, the jump rates must be uniquely determined from the state energies. The simplest choice of jump rates is then the Metropolis rates (Eq. (6)). Note that the jump rates must satisfy the principle of detailed balance [41], which ensures consistency with statistical mechanics

$$\frac{\Gamma(i \to j)}{\Gamma(j \to i)} = \exp[\beta (E_i - E_j)] \quad . \tag{10}$$

The jump rates of Eq. (6) ignore the possible existence of a barrier to be overcome between two nearest neighbor discrete states. The discretization ignores the possibility of vibrational motion around a minimum; thus the term "energy" E is

to be thought of as the potential energy U at a minimum, the "configurational part" of the potential energy. Similarly, the term "specific heat" henceforth refers to the configurational part of the measured specific heat, the socalled "excess specific heat" (in excess of the phonon contribution to the specific heat).

Step 4: Replacing complexity with randomness. The potential energy is a very complex function with numerous minima [30,42,63]. Therefore it is reasonable to replace the function E defined on the lattice with a function that is in some sense random. The idea of replacing complexity with randomness is old. In fact, this is the brilliant idea behind statistical mechanics: Any system with many degrees of freedom is extremely complex; in view of this one simply assumes that at a fixed energy any randomly chosen state is as likely as any other (the microcanonical ensemble). The basic idea is that some phenomena occurring in a specific complex system are typical of those that occur in most systems chosen randomly out of an ensemble of possible systems. If this is so, the study of random systems tells us what to expect for particular complex systems [69]. Motion in random potentials has been studied extensively in various contexts [48,70,71]. In discretizing such a model one often chooses the discretization length a equal to the correlation length of the random function and assumes that correlations beyond a may be ignored [71]. When this is done for the random walk model, the values of the potential are assumed to be uncorrelated from point to point on the d-

dimensional cubic lattice. In this approximation the model is fully specified by the energy probability distribution, the "density of states" $n(E)$.

Step 5: The assumption of cooperativity. A region contains many molecules and thus $d \gg 1$. Any system with many degrees of freedom has a density of states that can be written $n(E) = Ce^{S(E)}$ where the entropy as function of energy, $S(E)$, at relevant energies [72] obeys

$$\frac{\partial S}{\partial E} > 0 \quad ; \quad \frac{\partial^2 S}{\partial E^2} < 0 \quad . \tag{11}$$

The Gaussian Eq. (4) obeys Eq. (11), but only for negative energies. At any temperature, however, negative energies are most likely for the Gaussian and therefore it is permissible.

The assumption of a Gaussian density of states concludes the "derivation" of the random walk model. The model is completely specified by the parameters Γ_o, σ and d. The first two are "trivial" scaling parameters, so from a qualitative point of view only the dimension d is of interest.

In thermal equilibrium the probability of visiting any given site is given by the Boltzmann factor $\exp(-\beta E)$. Combining this with the Gaussian density of states Eq. (4), one finds for the equilibrium energy probability distribution $P_o(E) \propto \exp[-\beta E - E^2/(2\sigma^2)]$. By "completing the square" and normalizing, this may be rewritten

$$P_o(E) = \frac{1}{\sqrt{2\pi\sigma^2}} \exp\left[-\frac{(E-\bar{E})^2}{2\sigma^2}\right] , \quad \bar{E} = -\sigma^2\beta \quad . \qquad (12)$$

Clearly $\bar{E}$ is the average energy, which is also the most likely energy. The equilibrium specific heat, c_o, is given by

$$c_o \equiv \frac{d\bar{E}}{dT} = \frac{\sigma^2}{k_B T^2} \quad . \qquad (13)$$

Equation (13) may be derived directly from Einstein's expression, $c_o = \langle (\Delta E)^2 \rangle / (k_B T^2)$, since the Gaussian distribution Eq. (12) implies $\langle (\Delta E)^2 \rangle = \sigma^2$. The equilibrium specific heat increases towards infinity as the temperature goes to zero. While this cannot be true right down to zero temperature, there is for most supercooled liquids a tendency for the configurational specific heat to increase as the temperature decreases [2,38].

The random walk model was originally proposed by analogy to transport and relaxation of charge excitations in random organic solids [49]. Here the jump rates Eq. (6) are the well-known Miller-Abrahams jump rates for electronic hopping [73]. There are some differences between the above "derivation" of the random walk model and Bässler's justification of the model. In Bässler's original picture, the experimental dependence of the glass transition temperature on the sample history was understood as an effect due to the density of states depending on the preparation conditions [45]. The above picture is much more static; by confining attention to the multi-dimensional region, the density of states reflects the discretization of the

potential energy and does not depend on the conditions of sample preparation. A further difference between the above approach and that of Bässler and coworkers is that cooperativity is emphasized here, implying $d \gg 1$, while the original random walk model considered elementary jump processes on a "molecular or weakly cooperative level" [49], implying that d is not **much** larger than one.

3. DERIVING THE ENERGY MASTER EQUATION FROM THE RANDOM WALK MODEL

In order to monitor the average energy during a cooling and subsequent glass transition in the random walk model, there is probably no other method than to solve the master equation numerically by taking time steps of order $1/\Gamma_o \sim 1ps$. Clearly, this procedure cannot be used for simulating realistic laboratory time scales of order minutes or hours. In this section an approximation to the random walk model is derived, which makes it possible to investigate the model on realistic time scales. The approximate equation, the "energy master equation", is an equation for the time-evolution of the energy probability distribution, $P(E,t)$, which ignores the spatial d-dimensional structure of the random walk model.

Consider the random walk model in many dimensions ($d \gg 1$) at

low temperatures ($k_BT \ll \sigma$) and long times $t \gg \tau_0$. Whenever $k_BT \ll \sigma$ the most likely states have energies close to $\overline{E} = -\sigma^2\beta \ll -\sigma$ (Eq. (12)), i. e., deep into the negative tail of the Gaussian. These states are very rare, but the relaxation properties of the random walk model are dominated by them at low temperatures. The distance between two low-energy states is large, and a transition between two such states consists of a long and complex path joining neighboring states. It is hard to calculate the transition rate, but it is physically obvious that the transition rate depends mainly on the maximum energy encountered on the path [74,75]. Thus, of all possible paths between two low-energy states, the most likely paths are those that have the lowest maximum energy. The value of this maximum energy is identified by **percolation theory** [70,74-76]: Imagine the sites of the lattice gradually being filled in order of increasing energy. At a certain filling rate, the site percolation threshold p_c, an infinite "percolation" cluster of marked sites appears. In two dimensions $p_c = 0.593$, while in three dimensions $p_c = 0.312$ [70]. In high dimensions one finds [76] $p_c \approx 1/(2d-1)$. The highest energy on the percolation cluster, the "percolation energy" E_c, is given by

$$\int_{-\infty}^{E_c} n(E)\, dE = p_c \quad . \tag{14}$$

The percolation energy E_c gives a good estimate of the largest energy met on an "optimal" path between two low-energy sites. We

thus surmise [74,75] that the effective transition rate from a low-energy site with energy E_i to another low energy site with energy E_j is given by the barrier $\Delta E=E_c-E_i$: $\Gamma(i\to j) \propto \exp[-\beta\Delta E]$. Note that this expression, despite being independent of E_j, satisfies the principle of detailed balance Eq. (10). There are many possible final states, but since each jump rate is given by the above expression, the total rate for jumps away from a site with energy E, $\Gamma(E)$ is

$$\Gamma(E) = \Gamma_o^* e^{-\beta(E_c-E)} . \qquad (15)$$

To determine Γ_o^* we view the percolation cluster as a one-dimensional path, where each site has on the average two neighbors belonging to the cluster. This naive point of view ignores the complicated fractal nature of the cluster, but it does become realistic in high dimensions where it leads [76] to the correct percolation threshold. Since E_c is the largest energy on the percolation cluster, sites with energy E_c will on the average have two neighbors with lower energy. Thus, the total rate for jumps away from such a site is on the average $2\Gamma_o$, plus some terms for jumps to the higher energy neighbors. These terms are unimportant at low temperatures, and thus the prefactor of Eq. (15) is given by

$$\Gamma_o^* = 2\,\Gamma_o . \qquad (16)$$

To arrive at the simplest possible approximate description,

the spatial structure of the lattice is completely ignored. Consequently, all final states are regarded as equally likely. In the region language this means that, once excited, a region has forgotten which state it came from. Thus, one arrives at the picture of Fig. 1 which was first proposed by Goldstein [39] and subsequently discussed in much more detail by Brawer [8,43].

The approximate master equation considers only one variable, the energy. If the rate for jumps away from the state with energy E_i is denoted by $\Gamma_i \equiv \Gamma(E_i)$, the master equation is

$$\frac{dP_i}{dt} = -\Gamma_i P_i + K \quad . \tag{17}$$

Since all final states are assumed to be equally probably the number K must be the same for all i. K may be calculated from the requirement of conservation of probability:

$$\sum_j \frac{dP_j}{dt} = \frac{d}{dt} \sum_j P_j = 0 \tag{18}$$

implies that $K = \frac{1}{N} \sum_j \Gamma_j P_j$ where N is the number of states.

Equation (17) thus becomes

$$\frac{dP_i}{dt} = -\Gamma_i P_i + \frac{1}{N} \sum_j \Gamma_j P_j \quad . \tag{19}$$

It is convenient to convert Eq. (19) into a continuous description. Let $P(E,t)$ denote the energy probability distribution as function of time. The probability of jumping into an energy around E is proportional to the density of

states, $n(E)$, and Eq. (17) becomes for a suitable number C

$$\frac{\partial P(E,t)}{\partial t} = -\Gamma(E)\,P(E,t) + C\,n(E) \quad . \tag{20}$$

C may be determined from the requirement of conservation of probability: Since $n(E)$ is normalized,

$$\int_{-\infty}^{\infty} \frac{\partial P(E',t)}{\partial t}\,dE' = 0 \tag{21}$$

implies that

$$C = \int_{-\infty}^{\infty} \Gamma(E')\,P(E',t)\,dE' \quad . \tag{22}$$

In Eqs. (21) and (22) all energies were counted, despite the fact that the physical picture breaks down for $E > E_c$. However, including the energies above E_c gives the simplest description and causes little change because these high energy states are very unlikely. Now, Eq. (20) becomes an integro-differential equation, "the energy master equation" (EME) [44],

$$\frac{\partial P(E,t)}{\partial t} = -\Gamma(E)\,P(E,t) + n(E)\int_{-\infty}^{\infty} \Gamma(E')\,P(E',t)\,dE' \quad . \tag{23}$$

The EME was first discussed as a model for the thermalization of photoexcited charge carriers in amorphous semiconductors [77,78]. In this case $n(E)$ is the density of trapping levels in the band gap and E_c is the mobility edge of the conduction band. An equation similar to, but more complicated than Eq. (23), was used by Brawer in 1984 [43]. Brawer's equation contains an extra entropy factor enumerating

the different paths from a particular state to the transition state. A related approach towards relaxation in viscous liquids was advocated by Robertson and coworkers [79]. Towards the end of the 1980's the discrete version of Eq. (23), Eq. (17), was studied as a model for the relaxation properties of Derrida's random energy model [32], and Eq. (23) was proposed as a model for the dynamics of viscous liquids and it was studied numerically through the glass transition [44]. Recently, Eq. (23) was used by Arkhipov and Bässler to describe the low-temperature regime of viscous liquids, assuming that the high-temperature regime is described by the random walk model [53].

The static equilibrium solution of the EME, $P_o(E)$, is given by

$$P_o(E) = Const. \frac{n(E)}{\Gamma(E)} \quad . \tag{24}$$

From Eq. (15) it follows that this is just the canonical probability, as required by statistical mechanics. The canonical ensemble is realized in a very simple way: All states are visited equally often, but the average time spent in a state with energy E, $1/\Gamma(E)$, is proportional to the Boltzmann factor $\exp(-\beta E)$, thus giving the canonical probabilities.

At any fixed temperature an initial non-equilibrium energy probability distribution will approach the equilibrium distribution. This is also the case if the temperature changes in time: At any given time the distribution approaches the equilibrium distribution corresponding to the temperature at that time. Upon continued cooling the system freezes [44], because

the time it takes to reach equilibrium becomes too large.

The numerical solution of the EME is based on a calculation of the relaxation of $P(E,t)$ towards the equilibrium solution $P_o(E)$ at a fixed temperature. The arbitrary thermal history problem is solved by stepping ahead in time sufficiently small time steps, changing the temperature at each time step to mimic the changing temperature. As always in numerical work, one starts by discretizing the problem. The energy axis is discretized into N evenly spaced energies, $E_1 < \ldots < E_N$. At low temperatures it is important to include large negative energies into the set of discrete energies, despite these lying far out into the Gaussian tail. If one defines $P_i \equiv P(E_i,t)/C_p$, $\Gamma_i \equiv \Gamma(E_i)$, and $n_i \equiv n(E_i)/C_n$, where the normalization constants C_p and C_n are determined so that

$$\sum_{j=1}^{N} P_j = 1 \quad ; \quad \sum_{j=1}^{N} n_j = 1 \quad , \tag{25}$$

the EME becomes upon discretization

$$\frac{dP_i}{dt} = -\Gamma_i P_i + n_i \sum_{j=1}^{N} \Gamma_j P_j \quad (i=1,..,N) \quad . \tag{26}$$

At any temperature this equation may be solved by Laplace transformation [43,80-83] (detailed in the Appendix).

4. COMPUTER SIMULATIONS

This section reports computer simulations of the random walk model and compares them to the EME predictions. Results for a continuous cooling and reheating are given, as well as a study of the time evolution of the energy probability distribution for relaxation towards equilibrium at a fixed temperature. Unfortunately, it is impossible to check the validity of the EME description where it is expected to apply best: at low temperatures and long times in many dimensions; this would require enormous computer capacity. All simulations were performed in two dimensions, and in experiments monitoring relaxation towards equilibrium the lowest temperature studied was $0.25\ \sigma/k_B$.

A numerical solution of the random walk model may be obtained by monitoring the motion of a single "particle" in time, the analog of a Monte Carlo simulation. However, this introduces considerably noise and it is much more efficient to solve the master equation Eq. (5) directly. At any given time the state of the systems is represented by the probabilities, P_i. In two dimensions any site has 4 neighbors so the maximum transition rate is $4\Gamma_o$ (Eq. (6)). In the simulations a time step of length $1/(4\Gamma_o)$ was chosen, and for each pair of neighboring sites, A and B, the probabilities were changed in the following way: If $\Delta E=E_A-E_B>0$, the probabilities are upgraded according to

$$\Delta P_A = -\frac{1}{4} P_A + \frac{1}{4} e^{-\beta \Delta E} P_B$$
$$\Delta P_B = -\Delta P_A \qquad (27)$$

Each site is upgraded four times according to Eq. (27) and each time the non-upgraded probabilities are used as P_A and P_B. This time-discretization of the differential master equation is quite crude, but at long times it is sufficiently accurate. The important thing is to ensure probability conservation in each time step. All the simulations reported below were in two dimensions with periodic boundary conditions.

Figure 2 shows the glass transition monitored via the "dynamic" specific heat during a cooling to zero temperature at a constant rate and a subsequent reheating at the same rate. The dynamic specific heat, C, is defined by

$$C = \frac{\frac{dE}{dt}}{\frac{dT}{dt}} \qquad (28)$$

The full curves give the results of the simulations of the random walk model, the dashed curves the EME predictions, and the dots indicate the thermal equilibrium specific heat (Eq. (13)). The subfigures (a) and (b) show cooling and reheating from $T=2\sigma/k_B$ to $T=0$ in the time $100/\Gamma_o$, while (c) and (d) shows the same in time $10,000/\Gamma_o$. As expected, the EME predictions work better in the latter case.

Figure 3 shows the frozen-in energy for the cooling, i. e.,

the energy at zero temperature, as function of the cooling rate. Again the full curve gives the results of the simulations and the dashed curve gives the EME prediction.

The figures 4 and 5 show the energy probability distribution during relaxation towards thermal equilibrium, starting in equilibrium at one temperature and suddenly changing the temperature. In figure 4 the temperature was suddenly lowered. Four snapshots are shown giving the simulation results (full curve) and the EME predictions (dashed curve). The dots indicate the equilibrium energy probability distribution which is approached as $t \to \infty$. There is a sliding approach towards this equilibrium distribution. This is not the case for a sudden change from a low temperature to a higher temperature (Fig. 5). Here a two-bump distribution occurs, a phenomenon that was predicted within the EME some time ago [82].

In Figs. 4 and 5 what happens is that most states with energy below a characteristic energy, E_d, are frozen, while those with $E > E_d$ almost immediately thermalize. The energy E_d, which is marked by the vertical line, is the "demarcation energy" that was first introduced by Arkhipov and coworkers in the theory for excited charge carrier thermalization in amorphous semiconductors [77]. At any time t, E_d is found by putting the EME relaxation rate $\Gamma(E)$ equal to $1/t$ (below T is the temperature during the relaxation process):

$$E_d(t) = E_c - k_B T \ln(\Gamma_o^* t) \quad . \tag{29}$$

5. THE GLASS TRANSITION ACCORDING TO THE ENERGY MASTER EQUATION

The experimental glass transition takes place when the liquid upon cooling falls out of equilibrium because the average relaxation time becomes large compared to the cooling time. The same thing happens in the random walk model, as illustrated in Fig. 2. The previous section showed that the EME gives a good fit to the random walk model. The glass transition was studied in the EME some time ago [44]. This section reviews the findings of Ref. 44 to discuss what to expect at the glass transition in the random walk model. A closer study of the glass transition in the random walk model is planned for another publication.

In the EME the system is completely characterized by the energy probability distribution, $P(E,t)$. At the glass transition temperature, T_g, $P(E,t)$ freezes and stop changing upon further cooling. Only in some cases is the frozen-in energy distribution equal to the equilibrium energy probability distribution at T_g. To understand this phenomenon it is convenient again to refer to the demarcation energy, E_d [44]. Here, E_d acquires a meaning slightly different than in Sec. 4: Suppose the liquid is cooled at a constant rate to zero temperature in a time t_c, starting at equilibrium at some high temperature where the average relaxation time is much smaller than t_c. At any time during the cooling, the demarcation energy is the energy separating non-frozen states from the states that

are frozen **from that time on**. If t_L is the time left before zero temperature is reached, E_d is given by $E_d(t)=E_c-k_BT(t)\ln(\Gamma_o^* t_L)$. In realistic cases the glass transition takes place at a t_L which is of the same order of magnitude as t_c and much larger than $1/\Gamma_o^*$. Since t_L in the expression for the demarcation energy enters only in a logarithm, t_L may to a good approximation be replaced by the total cooling time, t_c:

$$E_d(t) = E_c-k_BT(t)\ln(\Gamma_o^* t_c) \quad . \tag{30}$$

Note that $E_d(t)$ increases with time during the cooling, whereas in Sec. 4 it decreased with time. In thermal equilibrium the energy probability distribution is a Gaussian centered around $\overline{E}(T)$. As the temperature is lowered, the Gaussian is displaced towards lower energies while at the same time $E_d(t)$ increases. When the Gaussian meets $E_d(t)$ the glass transition takes place [44]. This happens when $\overline{E}=E_d$. For the system with constant specific heat ck_B studied in Ref. 44, corresponding to $n(E)\propto E^{c-1}$, $0<E<\infty$, one has $\overline{E}(T)=k_BcT$ and the glass transition temperature is given by

$$k_B T_g = \frac{E_c}{c + \ln(\Gamma_o^* t_c)} \quad . \tag{31}$$

A linear relationship between $1/T_g$ and the logarithm of the cooling time is often observed in experiment [84].

For the freezing of the energy probability distribution there are two different scenarios, depending on the rate of change with temperature of E_d and $\bar{E}$ respectively. In the model studied in Ref. 44 $d\bar{E}/dT = ck_B$ and $dE_d/dT = -k_B \ln(\Gamma_o^* t_c)$. The case when E_d changes much faster than $\bar{E}$ was referred to as a "slow" glass transition, since it requires long cooling times: $\ln(\Gamma_o^* t_c) \gg c$. In this case the equilibrium Gaussian almost doesn't move at all when the demarcation energy passes it and freezes-in the energies. Thus, the frozen-in energy distribution, $P_f(E)$, is close to that corresponding to thermal equilibrium at $T = T_g$:

$$P_f(E) \approx \frac{1}{\sqrt{2\pi \langle (\Delta E)^2 \rangle}} \exp\left[-\frac{(E - E_g)^2}{2\langle (\Delta E)^2 \rangle} \right] , \tag{32}$$

where $E_g = ck_B T_g$ and $\langle (\Delta E)^2 \rangle = ck_B^2 T_g^2$. The other limiting case is that of a "fast" glass transition when $\ln(\Gamma_o^* t_c) \ll c$. Here, the demarcation energy moves very slowly compared to the Gaussian, and is almost constant during the glass transition. To determine $P_f(E)$

consider the energy fluctuations of a single region. As long as its energy is above the demarcation energy, the region "jumps" many times between the high-energy common states . Sooner or later, however, the region ends up in a state below E_d, or just above E_d, being subsequently frozen when E_d passes. As for all other jumps, this last jump hits an energy with a probability proportional to the density of states. Around E_g the density of states is proportional to $\exp[E/(k_B T_g)]$, so the normalized $P_f(E)$ is roughly given by

$$P_f(E) = \begin{cases} \frac{1}{k_B T_g} \exp\left[\frac{(E-E_g)}{k_B T_g}\right] & , \; E < E_g \\ 0 & , \; E > E_g \; . \end{cases} \qquad (33)$$

In Ref. 44 the predicted exponential increase of $P_f(E)$ below E_g was confirmed in the numerical solution of the master equation; however above E_g $P_f(E)$ was not seen to drop discontinuously to zero, but rather to follow a Gaussian decay.

The conclusion from the above is that, in general, one cannot expect at glass merely to have the structure of the equilibrium liquid at $T=T_g$. The average frozen-in energy is equal to the average energy of the equilibrium liquid at T_g, but the **distribution** of energies in the glass may be quite different from that corresponding to the equilibrium liquid. Any physical property which is a function of the region energy will in the

glass, if it depends linearly on E for the relevant energies, depending on the cooling rate be distributed according to a Gaussian or an exponential. Along these lines it has been argued that amorphous semiconductors prepared by a fast glass transition are likely to have exponential band tails of localized states [85].

It is convenient to define a number that distinguishes between the two types of glass transitions. This number, denoted by the greek letter iota ι, is the absolute value of the ratio between the change in the average energy and the change in the demarcation energy at the glass transition:

$$\iota = \left| \frac{d\bar{E}}{dE_d} \right| (T_g) \quad . \tag{34}$$

"Slow" glass transitions correspond to having $\iota \ll 1$ while "fast" glass transitions correspond to $\iota \gg 1$.

We now proceed to calculate the ι-parameter for the random walk model from the approximate EME description. In the random walk model the average energy is given by Eq. (12), $\bar{E}=-\sigma^2/(k_BT)$. The equation determining T_g, $E_d=\bar{E}$, is

$E_c-k_BT_g\ln(\Gamma_o^* t_c)=-\sigma^2/(k_BT_g)$, or

$$\ln(\Gamma_o^* t_c)\,(k_BT_g)^2 - E_c(k_BT_g) - \sigma^2 = 0 \quad . \tag{35}$$

The positive solution of this equation is

$$k_B T_g = \frac{E_c + \sqrt{E_c^2 + 4\sigma^2 \ln(\Gamma_o^* t_c)}}{2 \ln(\Gamma_o^* t_c)} \quad . \tag{36}$$

Since $d\bar{E}/dT=\sigma^2/(k_B T^2)$ and $dE_d/dT=-k_B \ln(\Gamma_o^* t_c)$ the iota-parameter is via Eqs. (34) and (35) given by

$$\begin{aligned} \imath &= \frac{\sigma^2}{(k_B T_g)^2 \ln(\Gamma_o^* t_c)} \\ &= 1 - \frac{E_c}{(k_B T_g) \ln(\Gamma_o^* t_c)} \quad . \end{aligned} \tag{37}$$

If the dimension $d>2$, the percolation energy E_c is negative; thus Eq. (36) implies

$$d>2: \quad \frac{E_c}{k_B T_g} = - \frac{2 \ln(\Gamma_o^* t_c)}{\sqrt{1 + 4 \frac{\sigma^2}{E_c^2} \ln(\Gamma_o^* t_c)} - 1} \quad . \tag{38}$$

When Eq. (38) is substituted into Eq. (37) one gets

$$d>2: \quad \imath = 1 + \frac{2}{\sqrt{1 + 4 \frac{\sigma^2}{E_c^2} \ln(\Gamma_o^* t_c)} - 1} \quad . \tag{39}$$

In the case $d=2$ E_c is positive and it is straightforward to show that the iota-parameter is given by

$$d=2: \quad \imath = 1 - \frac{2}{\sqrt{1 + 4 \frac{\sigma^2}{E_c^2} \ln(\Gamma_o^* t_c)} + 1} \quad . \tag{40}$$

Figure 6 gives the iota-parameter as function of the cooling times for $d=2,10,100,1000$.

The terminology of Ref. 44 referring to "slow" and "fast" glass transitions is not appropriate for the random walk model. For this model, as the cooling time goes to infinity, one finds $\iota \to 1$ in all dimensions; thus there are no "slow" glass transitions for slow cooling rates. On the other hand whenever $d > 2$ the glass transition is "fast" for sufficiently small cooling times; the case $d=2$ is peculiar in that the glass transition is "slow" for fast coolings! In view of this it is better to refer to glass transitions with $\iota \gg 1$ as "relaxational" glass transitions: These are the interesting cases where relaxation processes right at T_g result in a frozen-in energy distribution quite different from the equilibrium distribution. The cases when $\iota \ll 1$ may be referred to as "simple freezing" glass transitions; here the equilibrium energy distribution is simply frozen-in at T_g.

6. DISCUSSION

In this paper Bässler's random walk model for viscous liquids and the glass transition was re"derived" in Sec. 2. In Secs. 3 and 4, it was argued physically and illustrated by computer simulations that the energy master equation (EME) gives a good fit to the random walk model. Thereby, two at first sight

quite different approaches to the glass transition problem, that were proposed in the very same 1987 issue of Physical Review Letters [44,45], are unified. The below discussion is sectioned into parts, the first four a)-d) discuss the random walk model and its connection to the EME, while the last four e)-h) deal with the EME itself as a model for viscous liquids and the glass transition.

a) The random walk model in the present paper.

The physical justification of the random energy model was discussed in detail in Sec. 2. The most serious approximation made [29] is the partitioning of the liquid into non-interacting regions, an approximation that must be made to arrive at a tractable model. Replacing the deterministic equations of classical physics with stochastic equations seems more acceptable, though not without pitfalls [67,86]. A further approximation is the replacing of "complexity" by "randomness" [69]. This, in conjunction with the discretization of state space lead to the model of a random walk on a lattice with random energies. Models involving random walks in random environments ("rugged" energy landscapes) have been used in many contexts [48,70,75,86-91], and this type of models is becoming a paradigm for describing non-crystalline materials. In formulating a model of this type one is lead to ask whether the energy minima or the energy maxima should vary randomly, or both. The random walk model gives a simple and beautiful solution to this dilemma: No states are appointed "maxima" or "minima". All states are equal, but the higher-energy states become part of the paths between the populated, but rare, low-energy states. The assumption of

Gaussianly random energies is the simplest choice, and it also leads to an equilibrium specific heat which increases with decreasing temperature, as seen in experiment. The above mentioned properties of Bässler's random walk model indicate that it should be regarded as the "canonical" phenomenological model for viscous liquids and the glass transition.

Following the ideas of Derrida's "random energy model" [32] it is possible to build the Kauzmann paradox into the model by assuming that the Gaussian energy distribution is truncated at some low energy [92]. This, however, has not been attempted here, because such a "truncated" random walk model does not reproduce the experimental correlation between the Kauzmann temperature and the T_o of the VFT-law Eq. (2).

The random walk model contains three parameters. There are two scaling parameters, the width of the Gaussian σ and the microscopic time τ_o. The third parameter is the dimensionless state space dimension, d. For a qualitative discussion of the model there is thus only one relevant parameter, d; in this sense the model is also very simple.

b) A comparison to the original approach of Bässler and coworkers.

Bässler and coworkers [45,46] justified the Gaussian density of states by reference to the central-limit theorem, assuming that the region energy is a sum of a large number of independent contributions. However, one might similarly argue that **any** macroscopic system has a Gaussian density of states, implying that any such system has a specific heat varying with temperature

as $\propto T^{-2}$, which is clearly incorrect. In the present paper the Gaussian is an ad hoc assumption that is not sought justified beyond the fact that it gives a "thermodynamic" density of states. A further difference is that Bässler and coworkers assumed that the density of states fluctuates in time. This justified the use of Metropolis dynamics, since the "particle" awaits a favorable time for jumping where the barrier to be overcome is negligible. Here, the density of states is assumed constant and time-independent. This difference in the two approaches means that the present work cannot maintain the original interpretation of the fact that T_g depends on sample history. This fact was explained [45] as a logical consequence of the fact that the density of states depends on preparation conditions. Even for a constant density of states, however, does the glass transition temperature depend on sample history, so this is not a serious objection to the present approach.

The most elaborate version of the Bässler model was given in a recent paper by Arkhipov and Bässler [53]. They distinguish between a high-temperature regime described by the random walk model and a low-temperature regime described by the EME. The present work fully confirms this picture. Here, however, the random walk model is assumed to be the underlying model at all temperatures.

c) From the random walk model to the EME.

A number of models for the glass transition have previously emphasized the importance of percolation [13,40,94-96], but in different contexts than the present. At low temperatures the

populated states of the random walk model are rare low-energy states, and the transitions between states far apart follow the optimal paths, the ones that have the lowest maximum energy. The distance between two low-energy states is large and the maximum barrier of an optimal path is the percolation energy defined in terms of the site percolation threshold (Eq. (14)). In effect, the random walk model is at low temperatures regarded as consisting of states (=the deep minima) separated by barriers of the same height. The random walk model effectively reduces to a model of the "trapping" type (used, e. g., in the description of the trapping of electrons in amorphous semiconductors). Interestingly, it has previously been noted that the predictions of the trapping type random walk models are almost indistinguishable from the predictions of the EME [97,98].

The percolation energy makes it possible to distinguish two temperature regimes for the random walk model, a high-temperature regime opposed to the low-temperature regime where $\overline{E}(T) << E_c$. In the high-temperature regime the most likely states usually have one or more neighbors with a lower energy and these states thus have a very short "lifetime". In the low-temperature regime typical populated states are surrounded by states all of which have a higher energy. Only well into the low-temperature regime does the approximate EME description apply. This picture, which applies only for $d>2$ (for $d=2$ there is no high-temperature regime), is close to that recently advocated in general terms by Hunt [13,95]. He predicts that viscous liquids have a high-temperature regime described by effective-medium type theories

and a low-temperature regime where percolation effects dominate. A two regime picture also comes out of the mode-coupling theory [26], but in a different context.

The low-energy states could be thought of as effectively including a number of relatively low-energy neighboring states, thus forming rather complex low energy "basins" in agreement with the ideas of Stillinger and Weber [63,64] and Angell [11,30]. The complexity of the basins implies that considerable entropy resides inside each basin [11,93]. Note that this picture of complex minima derives from a model where neighboring energies are completely uncorrelated.

A transition between two low-energy states is a complex sequence of steps. Such a transition involves an element of **cooperativity** [8,29] in the sense that an optimal sequence of events have to be successfully traversed in order to have a transition. Thus, at low temperatures the random walk model contains both cooperativity and heterogeneity, the two factors identified by Scherer [29] as being important for any realistic model of viscous liquids. The random walk model also conforms to the thoughts of Goldstein in 1969, expressing a firm belief that, "when all is said and done, the existence of potential energy barriers large compared to the thermal energy are intrinsic to the occurrence of the glassy state, and dominate flow, at least at low temperatures" [42].

The approximate EME description of the random walk model ignores the spatial structure of the state space, the only trace left being the d-dependence of the percolation energy. In the limit of large d this is not unrealistic, since there are many

deep energy minima available not too far from a given minimum. Consequently, transitions to all states were allowed with equal probability in the EME.

d) Computer simulations: Comparing the random walk model to the EME predictions.

The approximate EME description makes it possible to find the predictions of the random walk model for realistic long times. This involves a numerical implementation of the analytic EME solution valid for the approach to thermal equilibrium at a fixed temperature (Appendix). In order to check the validity of the EME approximation computer simulations were carried out (Sec. 4). The EME is expected only to be valid in many dimensions at low temperatures and long times, a regime that unfortunately cannot be studied by even the fastest computers because of two problems: At low temperatures the most likely states are very rare so enormous lattices are needed; also the relaxation times are extremely long. Instead, the simulations were carried out in two dimensions only and at moderate temperatures. Despite this, the computer simulations revealed a rather good agreement with the EME predictions. A numerical study of thermalization in the random walk model was previously performed by Bässler and coworkers, starting in equilibrium at infinite temperature [99]. In Figs. 4 and 5 of the present paper, the thermalization was studied going from one finite to another finite temperature. A surprising thing happens in the more exotic case going from a low to a high temperature (Fig. 5) where a two-bump structure appears at intermediate times, a phenomenon that is reproduced by the EME. Thus, if the random walk model is realistic, one may induce

a "dynamically generated phase separation" in a glass by the following procedure: Anneal the glass for a very long time at a relatively low temperature to approach equilibrium, then increase the temperature and finally quench the glass after the right amount of time in order to catch the glass in a state corresponding to Fig. 5c.

The rest of this section deals with the EME on its own right.

e) The EME as the simplest possible truly cooperative master equation, "derived" from the non-Arrhenius temperature dependence of the average relaxation time.

Since most simple models involving a distribution of energy barriers give an average relaxation time $\tau(T)$ with an apparent activation energy that **decreases** with decreasing temperature, the observed non-Arrhenius $\tau(T)$ must contain an important clue to the construction of a phenomenological model. Assuming that the activation entropy plays little role we write

$$\tau(T) = \tau_o \, e^{\frac{\Delta E(T)}{k_B T}} \quad . \tag{41}$$

Experiments imply that $\Delta E(T)$ increases as the temperature decreases. The simplest way to explain this is as follows: $\Delta E(T)$ is the difference between the barrier to be overcome and the most likely region energy. If a region contains many molecules ("cooperativity") the most likely energy is by general thermodynamic principles close to the average energy $\overline{E}(T)$. If furthermore the barrier is assumed to be constant, $=E_c$, one has

$$\Delta E(T) = E_c - \overline{E}(T) \quad . \tag{42}$$

In the random walk model one thus finds $\Delta E(T) = E_c + \sigma^2/(k_B T)$, leading to $\tau(T) = \tau_o \exp[\sigma^2/(k_B T)^2 + E_c/(k_B T)]$ - a minor modification of Bässler's expression (Eq. (3)). Since $\overline{E}(T)$ decreases with decreasing temperature the barrier increases. This simple idea is the physical background for the EME: Eq. (42) motivates Eq. (15) and to derive the EME one just needs the further assumption - again the simplest possible - that, once excited into the transition state, a region may end up in any randomly chosen other state. This assumption means that an excitation must be a complete reordering of the region molecules, and thus the EME is truly cooperative.

f) The EME as the simplest master equation conforming to the Goldstein-Brawer picture (Fig. 1).

In an interesting paper from 1972 [39] Goldstein proposed a picture of viscous flow where the transition state is the "high-temperature, more-fluid, liquid usually studied by theorists". Once excited into this common transition state - being totally different from the potential energy minimum which the region was excited from - the only reasonable assumption is that any other lower energy state can be reached. In the EME these other states are all reached with equal probability. Thus, from Goldstein's ideas [39,42] one is lead almost automatically to the EME. Goldstein, however, did not formulate any master equation; a master equation in the spirit of his ideas was first set up by Brawer in 1984 [8,43]. His model is more detailed than

Goldstein's and the master equation is therefore also more complex than the EME. In the 1985 version of Brawer's model [8] a region has K volume elements, each of which has two states: a low-density (and high-energy) state and a high-density (and low-energy) state. The energy is a function of the average region density. If a certain fraction of the K volume elements are excited into the low-density state, a transition is allowed. In the model a transition is not just a simple jump, but a complex sequence of successful density changes involving a number of the volume elements, somewhat like a transition between two low-energy states in the random walk model.

g) The EME interpretation versus the standard interpretation of the activation energy.

Figure 7 sketches typical experimental results for the average relaxation time using an Arrhenius plot (full curves): There is a non-Arrhenius high-temperature regime for the equilibrium viscous liquid and an Arrhenius low-temperature regime (the glass). In the standard interpretation (Fig. 7a) the activation energy is the slope of the tangent (dashed line), which changes abruptly at the glass transition. The abrupt change is explained as being due to the fact that below T_g relaxation takes place in an essentially fixed structure, while above T_g the activation energy has an additional contribution from structural changes. Figure 7b gives the EME interpretation of data which follows directly from Eqs. (41) and (42). Here, the activation energy is the slope of the **secant** from $\tau(T)$ to τ_o. Thus, at $T=T_g$ the activation energy simply **stops changing**, because glassy

relaxation takes place in an essentially fixed structure.

h) A qualitative comparison of the EME and experiments.

The random walk model has been quantitatively successfully compared to experiments on a number of glass forming liquids [45,46,53]. We here proceed to argue that the EME itself, despite being very simple, qualitatively reproduces a large number of experimental observations, yields some new predictions, and also some "wrong" predictions. Most of the properties of the EME listed below will not be detailed here, but are straightforward to derive [82].

A. Qualitatively correct predictions of the EME:

1) The EME gives a qualitatively correct [8,43] temperature-dependence of the average relaxation time above and below T_g (Fig. 7);

2) The preexponential of $\tau(T)$ for glassy relaxation is predicted to be close τ_o, i.e., a phonon time [8,43];

3) A true Arrhenius behavior of $\tau(T)$ implies a zero region specific heat and thus no distributions of relaxation times [7,51,100]. If the region size is universal, as conjectured by Nemilov [101,102], there is a correlation between the magnitude of the "excess" specific heat (the configurational specific heat), the degree of non-Arrhenius behavior of $\tau(T)$ and the relaxation time distribution width [7,103,104];

4) If the region specific heat is regarded as roughly constant close to T_g, the EME predicts a proportionality between $1/T_g$ and the logarithm of the cooling time [84,105];

5) In the glassy state energy relaxation proceeds according to the EME with a logarithmic time dependence (compare Eq. (29)), "ln(t)-kinetics" [81,106,107], with a slower than logarithmic time dependence at both the initial and final stages. The logarithmic relaxation law is conventionally explained as being due to a "relaxation" of the relaxation rate itself [8,29,43,81,82,108], and the EME fully conforms to this picture.
6) For relaxation upon a sudden change in temperature an asymmetry is predicted between the two possible cases, a well-known phenomenon referred to as "nonlinearity" [8,29];
7) If one assumes a correlation between the region energy and its volume, which is necessary because the viscous liquid has a larger thermal expansion coefficient than the glass or crystal, the EME also gives predictions regarding the pressure dependence of the average relaxation time. Writing $\tau(p) \propto \exp[p\,\Delta V(p)]$ experiments imply that the activation volume increases as the pressure increases [109]. If $\Delta V(p) = V_c - \overline{V}(p)$ just as for the activation energy this observation is explained, since the region average volume must decrease with increasing pressure. Assuming a linear relation between region volume and energy, the normalized frequency-dependent isothermal compressibility must be equal to the normalized frequency-dependent specific heat, as predicted by Zwanzig [110]; there are some indications that this is obeyed in experiment [111]. Furthermore, for quantities uncorrelated with the region energy, it can be shown that the EME predicts a slight "decoupling" of their average relaxation time from that of the frequency-dependent specific heat, where the

average relaxation time for the latter becomes somewhat larger (Fig. 8). This is also the case experimentally [111].

B. New predictions of the EME:

1) At low temperatures the average relaxation time of the equilibrium viscous liquid is predicted to become Arrhenius with a preexponential equal to τ_o (of order 1 ps). Thus a change in sign of the curvature of the Arrhenius-plot $d^2\ln[\tau(T)]/d(T^{-1})^2$ is predicted. Similarly, a change in sign of $d^2\ln[\tau(p)]/dp^2$ at large pressure is predicted: This follows from the fact that a region must have a lowest energy state or a minimum volume. Such behavior has never been observed, although close to T_g the average relaxation time does become "Arrhenius", i.e., a straight line in the Arrhenius plot;

2) The EME gives detailed predictions regarding the nature of the asymmetry of relaxation upon sudden changes in temperature: For a sudden cooling from thermal equilibrium relaxation is predicted to proceed continuously (Fig. 4), while relaxation upon a sudden increase in temperature is peculiar, resulting in a two-bump energy probability distribution at intermediate times (Fig. 5). In the latter case, if the relaxation is interrupted by quenching to low temperatures, one ends up with a strange glass in which some regions have low energy and some have high energy, a "dynamically generated phase separation". Because of the energy-volume correlation such a glass would give an anomalous X-ray scattering signal. Nemilov has predicted a similar phenomenon on purely thermodynamic grounds [112];

3) The EME predicts that there are two different glass

transitions, "relaxational" (previously called "fast") glass transitions and "simple freezing" (previously called "slow") glass transitions. The latter type freezes-in the region energy probability distribution at T_g and the glass simply inherits the structure of the equilibrium liquid at this temperature. At a "relaxational" glass transition, relaxation processes right at T_g result in an frozen-in region energy distribution quite different from the equilibrium distribution. (Of course, glasses may be produced by a third kind of process, a "quench" to low temperatures in a time much shorter than the average relaxation time at the starting temperature - this process clearly results in a frozen-in region energy distribution that is equal to the equilibrium distribution at the starting temperature.)

C. "Wrong" predictions of the EME:

1) The Vogel-Fulcher law Eq. (2) is inconsistent with the EME which predicts a finite average relaxation time at all temperatures. Experimentally, however, deviations from this law occur for large viscosities where the date always exhibit a less dramatic temperature-dependence than predicted [20,29,51];

2) The Kauzmann paradox is also inconsistent with the EME which at all temperatures predicts a positive specific heat and thus no singularity. However, a suitably chosen region density of states (e.g., a truncated Gaussian [32,92]) easily reproduces the experimental configurational entropy;

3) The phenomenon β-relaxation is not predicted by the EME;

4) The Kohlrausch-Williams-Watts law (stretched exponentials) for the time-dependence of the energy relaxation is not reproduced by

the model. However, the EME does predict broad distributions of relaxation times.

These four points are places where the EME on the one hand does not reproduce the conventional picture of viscous liquids and glassy relaxation, but on the other hand is not inconsistent with experiment. The final point to be mentioned here is a more serious objection to the EME: If the correct non-Arrhenius behavior of $\tau(T)$ is to be reproduced by choosing a suitable $n(E)$ (possibly a non-Gaussian), the model predicts a peak of the imaginary part of the linear frequency-dependent specific heat [113] that is too broad. This conclusion seems to hold, despite the fact that only few measurements of this quantity have been published and that there is a considerable disagreement between the results of Christensen [114] and those of Birge and Nagel [115]. This disagreement between the EME and experiment means that the EME is too simple to be realistic. Preliminary work [116] indicates that it is possible solve this problem and still retain the region assumption and the assumption that the only important parameter is the region energy. This is done by the following extension of the EME. One introduces **two** densities of states, one numbering the minima and another essentially giving the entropy of each minimum. Thus, each minimum is a cluster of states that may be reached from each other by **not** exciting all the way to the energy E_c [117]. Besides giving greater flexibility to the EME-model, making it able to fit the frequency-dependent specific heat experiments, this approach also allows for the existence of β-relaxation as the process

associated with inter-minima transitions [117].

7. CONCLUSIONS

A "derivation" of Bässler's random walk model has been sketched, which emphasizes the potential importance of this model as a "canonical" or prototype phenomenological model for viscous liquids and the glass transition. The random walk model views relaxation as a consequence of activated transport within a multidimensional configuration space with a rugged energy landscape. It is probably the simplest model of this type. The "derivation" of Sec. 2 traces the random walk model back to Newton's equations for the molecules of one liquid region. However, the "derivation" is in no way exact, which is clear just from the fact that the crystalline state of much lower energy than the supercooled liquid states is absent from the model.

It has been shown that the EME gives a good approximate description of the energy fluctuations of the random walk model. The EME is solvable by a combination of analytical and numerical techniques (Appendix). This makes it possible to predict the behavior of the random walk model for an arbitrary temperature time variation at very long times. Independently of its justification from the random walk model, the EME may have a value of its own as a phenomenological model for viscous liquids and the glass transition. It incorporates true cooperativity and

is consistent with statistical mechanics, while still being simple and solvable for realistic laboratory time scales. It is noteworthy that even such a simple model leads to new predictions, like that there are two different types of glass transitions or that a well-annealed glass upon heating gives an anomalously large X-ray scattering at intermediate times before equilibrium is reached.

ACKNOWLEDGEMENTS

The author wishes to thank N. B. Olsen and T. Christensen for numerous enlightening discussions, and P. Borgstrom and I. H. Pedersen for technical assistance. This work was supported by the Danish Natural Science Research Council.

REFERENCES

1. G. Tammann, "Der Glaszustand" (L. Voss, Leipzig, 1933).
2. W. Kauzmann, Chem. Rev. **43**, 219 (1948).
3. R. O. Davies and G. O. Jones, Adv. Phys. **2**, 370 (1953).
4. M. Goldstein, in: "Modern Aspects of the Vitreous State", Ed. J. D. Mackenzie (Butterworths Scientific Publications Ltd., London, 1964), p. 90.
5. C. A. Angell and W. Sichina, Ann. N. Y. Acad. Sci. **279**, 53 (1976).
6. E. Donth, "Glasübergang" (Akademie-Verlag, Berlin, 1981).
7. C. A. Angell, in: "Relaxations in Complex Systems", Eds. K. L. Ngai and G. B. Wright (Govt. Printing Office, Washington, DC, 1985), p. 3.
8. S. Brawer, "Relaxation in Viscous Liquids and Glasses" (American Ceramic Society, Columbus, Ohio, 1985).
9. G. W. Scherer, "Relaxation in Glass and Composites" (Wiley, New York, 1986).
10. J. Jäckle, Rep. Progr. Phys. **49**, 171 (1986).
11. C. A. Angell, J. Non-Cryst. Solids **131-133**, 13 (1991).
12. F. Yonezawa, in "Solid State Physics", Ed. H. Ehrenreich and D. Turnbull (Acedemic Press, New York, 1991), Vol. 45, p. 179.
13. A. Hunt, J. Non-Cryst. Solids **160**, 183 (1993).
14. I. M. Hodge, J. Non-Cryst. Solids **169**, 211 (1994).
15. H. Rawson, "Properties and applications of glass" (Elsevier, Amsterdam, 1980).
16. C. A. Angell, J. Phys. Chem. **70**, 2793 (1966).

17. A. J. Kovacs, Fortschr. Hochpolymer.-Forsch. **3**, 394 (1963).

18. J. D. Ferry, "Viscoelastic Properties of Polymers", 3rd Ed. (Wiley, New York, 1980).

19. H. S. Chen, Rep. Progr. Phys. **43**, 353 (1980).

20. A. J. Barlow, J. Lamb, and A. J. Matheson, Proc. Roy. Soc. A **292**, 322 (1966).

21. G. Harrison, "The Dynamic Properties of Supercooled Liquids" (Academic Press, New York, 1976).

22. C. A. Angell, J. H. R. Clarke, and L. V. Woodcock, Adv. Chem. Phys. **48**, 397 (1981).

23. J.-P. Hansen, Physica A **201**, 138 (1993).

24. K. Binder and A. P. Young, Rev. Mod. Phys. **58**, 801 (1986),.

25. V. S. Dotsenko, Usp. Fiz. Nauk **163**, 1 (1993) [Physics Uspekhi **36**, 455 (1993)].

26. W. Götze and L. Sjögren, Rep. Progr. Phys. **55**, 241 (1992).

27. S. P. Das and G. F. Mazenko, Phys. Rev. A **34**, 2265 (1986).

28. Second International Discussion Meeting on Relaxations in Complex Systems (Alicante, 28 June - 8 July, 1993) [Proceedings published in Vols. **172-174** of J. Non-Cryst. Solids.]

29. G. W. Scherer, J. Non-Cryst. Solids **123**, 75 (1990).

30. C. A. Angell, J. Phys. Chem. Solids **49**, 863 (1988).

31. J. Jäckle, Mat. Res. Soc. Symp. Proc. **215**, 151 (1991).

32. B. Derrida, Phys. Rev. Lett. **45**, 79 (1980).

33. G. H. Fredrickson, Ann. Rev. Phys. Chem. **39**, 149 (1988).

34. T. A. Weber, G. H. Fredrickson, and F. H. Stillinger, Phys. Rev. B **34**, 7641 (1986).

35. J. H. Gibbs and E. A. DiMarzio, J. Chem. Phys. **28**, 373

(1958).

36. G. Adam and J. H. Gibbs, J. Chem. Phys. **43**, 139 (1965).

37. P. D. Gujrati and M. Goldstein, J. Chem. Phys. **74**, 2596 (1981).

38. C. A. Angell and K. J. Rao, J. Chem. Phys. **57**, 470 (1972).

39. M. Goldstein, Faraday Symp. Chem. Soc. **6**, 7 (1972).

40. G. S. Grest and M. H. Cohen, Adv. Chem. Phys. **48**, 455 (1981).

41. N. G. van Kampen, "Stochastic Processes in Physics and Chemistry" (North-Holland, Amsterdam, 1981).

42. M. Goldstein, J. Chem. Phys. **51**, 3728 (1969).

43. S. A. Brawer, J. Chem. Phys. **81**, 954 (1984).

44. J. C. Dyre, Phys. Rev. Lett. **58**, 792 (1987).

45. H. Bässler, Phys. Rev. Lett. **58**, 767 (1987).

46. R. Richert and H. Bässler, J. Phys.: Condens. Matter **2**, 2273 (1990).

47. J. W. Haus and K. W. Kehr, Phys. Rep. **150**, 263 (1987).

48. J. C. Dyre, Phys. Rev. B. **49**, 11709 (1994).

49. H. Bässler, in "Advances in Disordered Semiconductors", Vol. 2, Ed. H. Fritzsche and M. Pollak (World Scientific, Singapore, 1990), p. 491.

50. J. H. Simmons and P. B. Macedo, J. Res. Nat. Bureau Standards **75A**, 175 (1971).

51. H. Tweer, J. H. Simmons, and P. B. Macedo, J. Chem. Phys. **54**, 1952 (1971).

52. T. A. Litovitz, J. Chem. Phys. **20**, 1088 (1952).

53. V. I. Arkhipov and H. Bässler, J. Phys. Chem. **98**, 662 (1994).

54. A. Hunt, Int. J. Theoret. Phys. B **8**, 855 (1994).

55. W. Kauzmann, Rev. Mod. Phys. **14**, 12 (1942).

56. T. Alfrey, "Mechanical Properties of High Polymers" (Interscience Publishers, New York, 1948).

57. G. Williams, in: "Dielectric and Related Molecular Processes, Specialist Periodical Report, Vol. 2", Ed. M. Davies (Chem. Soc., London, 1975), p. 151.

58. E. Donth, J. Non-Cryst. Solids **53**, 325 (1982).

59. F. H. Stillinger, J. Chem. Phys. **89**, 6461 (1988).

60. R. V. Chamberlin, Phys. Rev. B **48**, 15638 (1993).

61. G. Wahnström, Phys. Rev. A **44**, 3752 (1991).

62. R. D. Mountain and D. Thirumalai, Phys. Rev. A **45**, R3380 (1992).

63. F. H. Stillinger and T. A. Weber, Science **225**, 983 (1984).

64. F. H. Stillinger, Phys. Rev. B **41**, 2409 (1990).

65. M. Doi and S. F. Edwards, "The Theory of Polymer Dynamics" (Clarendon, Oxford, 1986).

66. W. Hess and R. Klein, Adv. Phys. **32**, 173 (1983).

67. H. Löwen, J.-P. Hansen, and J.-N. Roux, Phys. Rev. A **44**, 1169 (1991).

68. H. Eyring, J. Chem. Phys. **4**, 283 (1936).

69. P. G. Wolynes, Acc. Chem. Res. **25**, 513 (1992).

70. M. B. Isichenko, Rev. Mod. Phys. **64**, 961 (1992).

71. S. Kirkpatrick, Rev. Mod. Phys. **45**, 574 (1973).

72. K. Huang, "Statistical Mechanics" (Wiley, New York, 1963).

73. A. Miller and E. Abrahams, Phys. Rev. **120**, 745 (1960).

74. V. Ambegaokar, B. I. Halperin, and J. S. Langer, Phys. Rev. B **4**, 2612 (1971).

75. B. I. Shklovskii and A. L. Efros, Zh. Eksp. Teor. Fiz. **60**, 867 (1971) [Sov. Phys. JETP **33**, 468 (1971)].

76. D. Stauffer and A. Aharony, "Introduction to Percolation Theory", 2nd Ed. (Taylor and Francis, London, 1992).

77. V. I. Arkhipov, M. S. Iovu, A. I. Rudenko, and S. D. Shutov, Phys. Status Solidi (a) **54**, 67 (1979).

78. J. Orenstein, M. A. Kastner, and V. Vaninov, Philos. Mag. B **46**, 23 (1982).

79. R. E. Robertson, R. Simha, and J. G. Curro, Macromolecules **17**, 911 (1984).

80. G. J. M. Koper and H. J. Hilhorst, Europhys. Lett. **3**, 1213 (1987).

81. E. I. Shakhnovich and A. M. Gutin, Europhys. Lett. **9**, 569 (1989).

82. J. C. Dyre, "Master Equation Approach to Viscous Liquids and the Glass Transition", (IMFUFA tekst nr. 154, Roskilde University, 1988).

83. G. Arfken, "Mathematical Methods for Physicists" (Academic Press, New York, 1985).

84. C. T. Moynihan, A. J. Easteal, M. A. DeBolt, J. Tucker, J. Am. Ceram. Soc. **59**, 12 (1976).

85. J. C. Dyre, Key Engineering Materials **13-15**, 501 (1987).

86. W. Tschöp and R. Schilling, Phys. Rev. E **48**, 4221 (1993).

87. J. C. Dyre, J. Appl. Phys. **64**, 2456 (1988).

88. H. Frauenfelder, S. G. Sligar, and P. G. Wolynes, Science **254**, 1598 (1991).

89. C. Aslangul, N. Pottier, and D. Saint-James, Physica A **164**, 52 (1990).

90. R. Tao, Phys. Rev. A **43**, 5284 (1991).

91. A. B. Kolomeisky and E. B. Kolomeisky, Phys. Rev. A **45**, R5327 (1992).

92. M. D. Bal'makov, Fiz. Khim. Stekla **12**, 527 (1986) [Sov. J. Glass Phys. Chem. **12**, 279 (1986)].

93. M. Goldstein, J. Chem. Phys. **64**, 4767 (1976).

94. Y. Hiwatari, J. Chem. Phys. **76**, 5502 (1982).

95. A. Hunt, Solid State Commun. **84**, 701 (1992).

96. M. F. Thorpe, J. Non-Cryst. Solids **57**, 355 (1983).

97. M. Silver, G. Schoenherr, and H. Baessler, Phys. Rev. Lett. **48**, 352 (1982).

98. H. Bässler, Progr. Colloid & Polymer Sci. **80**, 35 (1989).

99. B. Ries, H. Bässler, M. Grünewald, and B. Movaghar, Phys. Rev. B **37**, 5508 (1988).

100. A. R. Dexter and A. J. Matheson, Adv. Mol. Relax. Processes **2**, 251 (1972).

101. S. V. Nemilov, Fiz. Khim. Stekla **2**, 193 (1976) [Sov. J. Glass Phys. Chem. **2**, 187 (1976)].

102. S. V. Nemilov, Fiz. Khim. Stekla **4**, 129 (1978) [Sov. J. Glass Phys. Chem. **4**, 113 (1978)].

103. T. A. Vilgis, Phys. Rev. B **47**, 2882 (1993).

104. R. Böhmer, J. Non-Cryst. Solids **172-174**, 628 (1994).

105. G. M. Bartenev, "The Structure and Mechanical Properties of Inorganic glasses" (Wolters-Noordhoff, Groningen, 1970).

106. M. R. J. Gibbs, J. E. Evetts, and J. A. Leake, J. Mater. Sci. **18**, 278 (1983).

107. A. van den Beukel, S. van der Zwaag, and A. L. Mulder, Acta Metall. **32**, 1895 (1984).

108. O. V. Mazurin, J. Non-Cryst. Solids **25**, 130 (1977).

109. G. P. Johari and E. Whalley, Faraday Symp. Chem. Soc **6**, 23 (1972).

110. R. Zwanzig, J. Chem. Phys. **88**, 5831 (1988).

111. T. Christensen and N. B. Olsen, Phys. Rev. B. **49**, 15396 (1994); unpublished.

112. S. V. Nemilov, Fiz. Khim. Stekla **11**, 146 (1985) [Sov. J. Glass Phys. Chem. **11**, 97 (1985)].

113. K. D. Jensen, and J. Nielsen, unpublished.

114. T. Christensen, J. Phys. (Paris) Colloq. **46**, C8-635 (1985).

115. N. O. Birge and S. R. Nagel, Phys. Rev. Lett. **54**, 2674 (1985).

116. J. C. Dyre, unpublished.

117. V. Rosato and G. Williams, Adv. Mol. Relax. Processes **20**, 233 (1981).

APPENDIX: SOLVING THE ENERGY MASTER EQUATION

We first calculate how an initial non-equilibrium energy probability distribution at a fixed temperature converges to the canonical equilibrium distribution [43,79-82]. Working with the discrete version of the master equation, the Laplace transform of the function $P_i(t)$ appearing in Eq. (26), $\tilde{P}_i(s)$, is as usual defined [82] by

$$\tilde{P}_i(s) = \int_o^\infty P_i(t)\, e^{-st} dt \quad . \tag{A.1}$$

Since the Laplace transform of the time derivative of a function $f(t)$ is $s\tilde{f}(s) - f(0)$, Eq. (26) becomes upon Laplace transforming

$$s\tilde{P}_i(s) - P_i(0) = -\Gamma_i\, \tilde{P}_i(s) + n_i\, X(s) \quad , \tag{A.2}$$

where $X(s) = \sum_{j=1}^{N} \Gamma_j \tilde{P}_j(s)$. These equations determine $\tilde{P}_i(s)$ from a knowledge of the initial probabilities, $P_i(0)$. The probabilities at a later time are then calculated by the inverse Laplace transformation [82],

$$P_i(t) = \frac{1}{2\pi i} \int_{-i\infty}^{+i\infty} \tilde{P}_i(s)\, e^{st} ds \quad . \tag{A.3}$$

Isolating $\tilde{P}_i(s)$ from Eq. (A.2) leads to

$$\tilde{P}_i(s) = \frac{P_i(0)}{s+\Gamma_i} + \frac{n_i}{s+\Gamma_i} X(s) \quad . \qquad (A.4)$$

From this expression an equation for $X(s)$ is found by multiplying with Γ_i on each side and summing, leading to

$$X(s) = \sum_{i=1}^{N} \frac{\Gamma_i P_i(0)}{s+\Gamma_i} + X(s) \sum_{i=1}^{N} \frac{n_i \Gamma_i}{s+\Gamma_i} \quad , \qquad (A.5)$$

or

$$X(s) = \frac{\sum_{i=1}^{N} \frac{\Gamma_i P_i(0)}{s+\Gamma_i}}{1 - \sum_{i=1}^{N} \frac{n_i \Gamma_i}{s+\Gamma_i}} \quad . \qquad (A.6)$$

Since $\sum_{i=1}^{N} n_i = 1$ (Eq. (25)) the denominator may be rewritten

$$1 - \sum_{i=1}^{N} \frac{n_i(\Gamma_i+s-s)}{s+\Gamma_i} = s \sum_{i=1}^{N} \frac{n_i}{s+\Gamma_i} \quad . \qquad (A.7)$$

When substituted into Eqs. (A.6) and (A.4) this gives (changing the summation index from i to j)

$$\tilde{P}_i(s) = \frac{P_i(0)}{s+\Gamma_i} + \frac{n_i}{s(s+\Gamma_i)} \frac{\sum_{j=1}^{N} \frac{\Gamma_j P_j(0)}{s+\Gamma_j}}{\sum_{j=1}^{N} \frac{n_j}{s+\Gamma_j}} \quad . \qquad (A.8)$$

From Eq. (A.8) $P_i(t)$ may be calculated via Eq. (A.3), where the integration contour in the complex plane lies to the right of all poles of $\tilde{P}_i(s)$. The integral is evaluated by including an

infinitely large semicircle surrounding the left half-plane of the complex plane. This closes the integration contour and the residue theorem may be applied. There are N poles for each i which , due to the structure of the energy master equation, are the same for all $\tilde{P}_i(s)$ $(i=1,..,N)$. There is one pole at $s=0$. The apparent singularities at $s=-\Gamma_j$, however, are all "removable", i.e., not real singularities. If $j=i$ this follows from the fact that

$$\lim_{s\to-\Gamma_i} (s+\Gamma_i)\tilde{P}_i(s) = P_i(0) + \frac{n_i}{(-\Gamma_i)}\frac{\Gamma_i P_i(0)}{n_i} = 0 \quad , \tag{A.9}$$

while for $j\neq i$ it follows from

$$\lim_{s\to-\Gamma_j} (s+\Gamma_j)\tilde{P}_i(s) = 0 + 0\frac{\Gamma_j P_j(0)}{n_j} = 0 \quad . \tag{A.10}$$

Besides the $s=0$ pole there are poles whenever s obeys

$$\sum_{j=1}^{N} \frac{n_j}{s+\Gamma_j} = 0 \quad . \tag{A.11}$$

This equation has $N-1$ solutions, each of which is a negative real number. The solutions are conveniently denoted by $s=-\omega_k$ and numbered such that

$$\Gamma_k < \omega_k < \Gamma_{k+1} \quad (k=1,..,N-1) \quad . \tag{A.12}$$

The ω's are defined by

$$\sum_{j=1}^{N} \frac{n_j}{\Gamma_j - \omega_k} = 0 \qquad (k=1,..,N-1) \quad . \tag{A.13}$$

We next proceed to find the residues. At the pole $s=0$ the residue is given by

$$\lim_{s\to 0} s\,\tilde{P}_i(s) = 0 + \frac{n_i}{\Gamma_i} \frac{\sum_{j=1}^{N} P_j(0)}{\sum_{j=1}^{N} \frac{n_j}{\Gamma_j}} = \frac{\frac{n_i}{\Gamma_i}}{\sum_{j=1}^{N} \frac{n_j}{\Gamma_j}} \quad . \tag{A.14}$$

Since the quantity $n_i/\Gamma_i \propto n_i \exp(-\beta E_i)$ is proportional to the canonical equilibrium probability for the system being in state i, the pole at $s=0$ is simply the normalized equilibrium probability, $P_{o,i}$:

$$\lim_{s\to o} s\tilde{P}_i(s) = P_{o,i} \quad . \tag{A.15}$$

Using the rule that the residue of a function of the form $f(z)/g(z)$ at a simple zero for $g(z)$ at $z=z_o$ is $f(z_o)/g'(z_o)$, one finds for the residues at $s=-\omega_k$

$$\begin{aligned} \lim_{s\to -\omega_k} (s+\omega_k)\tilde{P}_i(s) &= 0\frac{P_i(0)}{\Gamma_i - \omega_k} + \\ &+ \frac{n_i}{(-\omega_k)(\Gamma_i - \omega_k)} \frac{\sum_{j=1}^{N} \frac{\Gamma_j P_j(0)}{\Gamma_j - \omega_k}}{\sum_{j=1}^{N} \frac{(-n_j)}{(\Gamma_j - \omega_k)^2}} \\ &= \frac{n_i}{\omega_k(\Gamma_i - \omega_k)} A_k \quad . \end{aligned} \tag{A.16}$$

where

$$A_k = \frac{\sum_{j=1}^{N} \frac{\Gamma_j P_j(0)}{\Gamma_j - \omega_k}}{\sum_{j=1}^{N} \frac{n_j}{(\Gamma_j - \omega_k)^2}} \quad (k=1,..,N-1) \quad . \qquad (A.17)$$

Having determined the residues the integral Eq. (A.3) is now easily calculated by the residue theorem:

$$P_i(t) = P_{o,i} + \sum_{k=1}^{N-1} \frac{n_i}{\omega_k(\Gamma_i - \omega_k)} A_k \, e^{-\omega_k t} \quad . \qquad (A.18)$$

Clearly, the solution converges to the equilibrium solution as $t \to \infty$. The ω_k's play the role of characteristic relaxation rates. Note that conservation of probability is ensured at all times by virtue of Eq. (A.13).

The equations (A.13), (A.17) and (A.18) give the solution of the energy master equation at a fixed temperature. In the numerical implementation the ω's are determined from Eq. (A.13) by the bisection method. Depending on the numerical precision large numerical errors may arise from the term $1/(\Gamma_k - \omega_k)$ in Eqs. (A.17) and (A.18) at low energies where ω_k is extremely close to Γ_k; in this case one may use Eq. (A.13) to approximate as follows

$$\frac{1}{\Gamma_k - \omega_k} \approx -\frac{1}{n_k} \sum_{j=1, j \neq k}^{N} \frac{n_j}{\Gamma_j - \omega_k} \quad . \qquad (A.19)$$

Another problem that may arise is overflow. In the present work both these numerical problems were avoided by using the 80 bit floating point "extended" data type of Turbo Pascal that utilizes a remarkable capacity of the 486 Intel processor. If this

possibility is not available, overflow problems may be avoided by the following procedure: The numbers $P_j, P_j(0), n_j, \Gamma_k, \omega_k$ are each represented by their logarithm. Each sum appearing in Eqs. (A.13), (A.17) and (A.18) is evaluated by first identifying the leading term and then factorizing it. There remains a sum of terms less than one, each term being a product which is evaluated as, e.g., $ab=\exp[\ln(a)+\ln(b)]$.

The master equation may be solved accurately numerically at arbitrary long times at a fixed temperature. If the temperature changes in time, the above method is applied for time steps small enough that the temperature may be considered constant. In the solutions of the master equation plotted in Figs. 2-5 the energy axis was discretized into energies spaced 0.1σ apart spanning an energy interval of 10 σ, suitably placed on the energy axis depending on the problem. The solutions plotted in Fig. 2 were obtained from 200 time steps where the temperature is changed in each step. In two dimensions the percolation energy (Eq. (14)) is given by $E_c=0.2345\sigma$.

FIGURE CAPTIONS

Fig. 1: The Goldstein-Brawer picture of a "flow event" in a viscous liquid [8,39,43]. The figure illustrates the excitation from one "state", i. e., a potential energy minimum for the molecules in a region of the liquid, to another state, the vertical axis being the energy axis. In Goldstein's model the transition state (black) is identified with the high-temperature, more-fluid, liquid [39]; Brawer identifies it with a low-density state giving room for the molecules to rearrange [8,43]. In the approximate energy master equation (EME) description of Bässler's random walk model, the energy of the transition state is identified with the energy at the percolation threshold (Eq. (14)). The Goldstein-Brawer picture leads directly to the EME (Eq. (23)) if it is assumed that, once excited into the transition state, the region has forgotten which state it came from and ends up in a randomly chosen state.

Fig. 2: The glass transition in the random walk model in two dimensions (full curves) monitored via the specific heat during a cooling at constant rate to zero temperature, and the subsequent "melting" upon reheating at the same rate. The dashed curves give the EME predictions, and the dots mark the thermal equilibrium specific heat (Eq. (13)). (a) shows the specific heat [k_B] as function of temperature T [σ/k_B] for cooling in the time t=100 [$1/\Gamma_o$] starting from equilibrium at T=2; (b) gives the reheating data. The subfigures (c) and (d) are similar

but with cooling and reheating time t=10000. The random walk model data were obtained by averaging over 10 simulations of a 50X50 lattice. The EME was solved by the method detailed in the Appendix. Clearly, the EME works better for the slower cooling rate.

Fig. 3: The average frozen-in energy [σ] at zero temperature as function of the logarithm (base 10) of the cooling time [$1/\Gamma_o$] for coolings starting from equilibrium at T=2 [σ/k_B]. The full curve gives the results from simulations of the random walk model (10 averages of a 50X50 lattice), and the dashed curve gives the EME predictions which are best at long cooling times.

Fig. 4: Relaxation towards thermal equilibrium of the energy probability distribution, $P(E,t)$, upon a sudden lowering of the temperature starting at equilibrium. The figure shows 4 snapshots of $P(E,t)$ (full curves: simulations of the random walk model, dashed curves: the EME predictions) starting at T=2 [σ/k_B] lowering the temperature at t=0 to T=0.357 at the following times [$1/\Gamma_o$]: (a) t=5, (b) t=184, (c) t=5953, (d) t=80752. The vertical line marks the "demarcation energy" E_d defined at time t in the EME by Eq. (29). In the approximate EME description most states with $E<E_d$ have not jumped since t=0. As $t\to\infty$ $E_d\to-\infty$ and thermal equilibrium is reached. For

the subfigures (a)-(c) the full curves give results for averages of 10 simulations of a 1000X1000 lattice, while for (d) only one simulation was possible.

Fig. 5: Relaxation towards thermal equilibrium of the energy probability distribution, $P(E,t)$, upon a sudden raising of the temperature starting at equilibrium. The figure shows 4 snapshots of $P(E,t)$ (full curves: simulations of the random walk model, dashed curves: the EME predictions) starting at T=0.25 $[\sigma/k_B]$ at time t=0 and subsequently annealing at the temperature T=1.0. The snapshots are taken at the following times $[1/\Gamma_o]$: (a) t=2, (b) t=8, (c) t=25, (d) t=126. The vertical line marks the "demarcation energy" E_d defined at time t in the EME by Eq. (29). In the approximate EME description most states with $E<E_d$ have not jumped since t=0. As $t\to\infty$ $E_d\to-\infty$ and thermal equilibrium is reached. The full curves give results for averages of 20 simulations of a 1000X1000 lattice. In Figs. 4 and 5 very large lattices are needed to minimize the statistical fluctuations and to be able to move deep into the Gaussian tail. The noise seen at low energies is statistical noise due to the fact that there are very few states in the deep Gaussian tail. The two-bump distribution that appears at intermediate times during the annealing reflects that, once a populated state has jumped away from its low energy, it almost immediately thermalizes. This is because there are many high energy states which are easy to find. Since the region energy correlates with

the volume (the liquids has a thermal expansion coefficient which is larger than that of the glass), the model predicts that there is an anomalously large X-ray scattering at the intermediate times during the annealing, corresponding to subfigure (c).

Fig. 6: The iota-parameter ι (Eqs. (39) and (40)) characterizing the glass transition in the random walk model for different dimensions (d=2,10,100,1000) as function of cooling time according to the EME. If $\iota \ll 1$ the transition is a "simple freezing" glass transition, where the energy probability distribution of the glass is the equilibrium distribution at T_g frozen-in almost unmodified. In the other limit, $\iota \gg 1$, the transition is a "relaxational" glass transition, where relaxations right at the transition considerably deforms the equilibrium energy probability; as a result the glass does **not** acquire a structure corresponding to the equilibrium liquid at T_g. As $t \to \infty$ one ends up in the mixed case $\iota = 1$ where there is some relaxation at T_g. The difference between $d=2$ and $d>2$ arises from the fact that only in two dimensions is the percolation energy positive.

Fig. 7: Standard interpretation of the activation energy (a) compared to the interpretation underlying the random walk model and the EME (b). Both figures show an Arrhenius plot of the same typical average relaxation time data for the supercooled liquid (non-Arrhenius part, $T > T_g$) and for the glass (Arrhenius part,

$T<T_g$). In the Fig. 7a the activation energy is the slope of the **tangent**, which changes discontinuously at T_g. In Fig. 7b the activation energy is instead the slope of the **secant** drawn to the microscopic time. In both cases one also finds that the activation energy increases as the temperature decreases; but in (b) what happens at the glass transition is simply that the activation energy stops increasing and becomes constant.

Fig. 8: Decoupling of thermal relaxation times from other relaxation times according to the EME (putting here E_c=0). The full curve gives the loss peak frequency calculated from the auto-correlation function for a quantity that is uncorrelated to the energy. The dashed curve is the specific heat loss peak frequency [113,116]. The figure shows that there is a slight slowing down of thermal relaxation compared to other relaxations, an effect that has been seen in experiment [111].

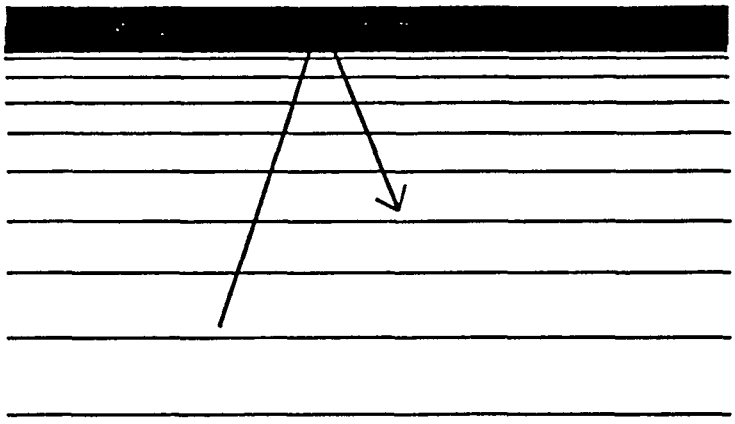

Fig. 1

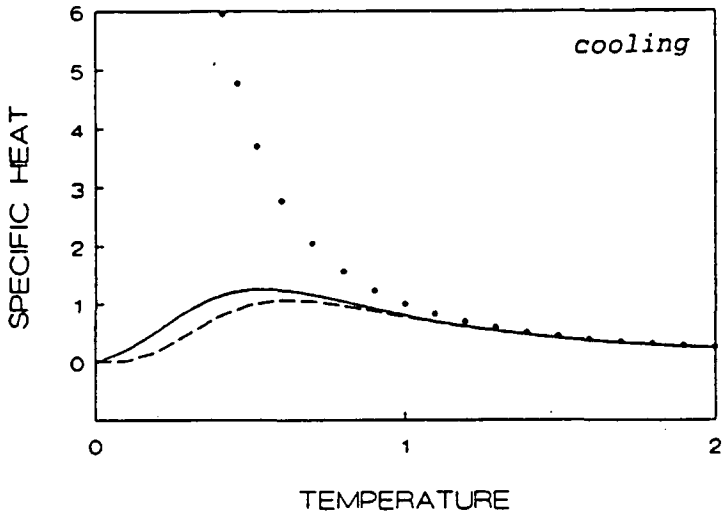
cooling
SPECIFIC HEAT
6
5
4
3
2
1
0
0
1
2
TEMPERATURE

Fig. 2a

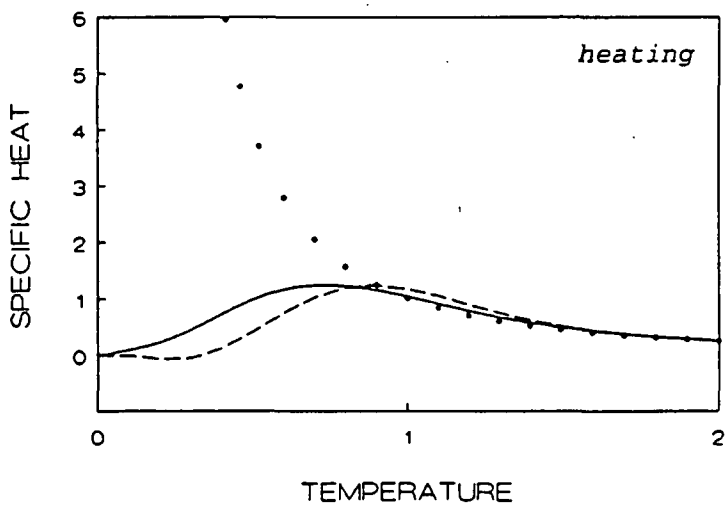
heating
SPECIFIC HEAT
6
5
4
3
2
1
0
0
1
2
TEMPERATURE

Fig. 2b

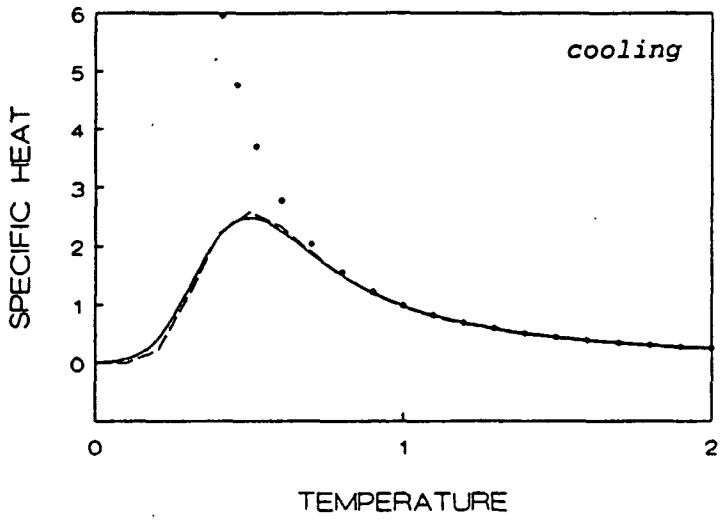
cooling
SPECIFIC HEAT
TEMPERATURE
0
1
2
3
4
5
6

Fig. 2c

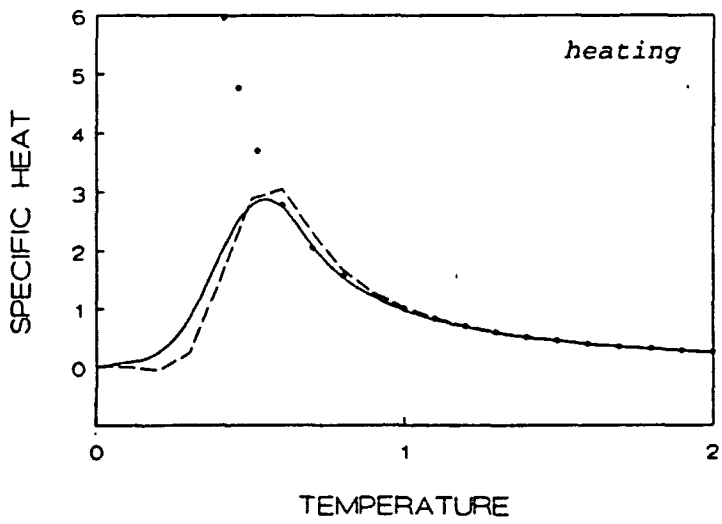
heating
SPECIFIC HEAT
TEMPERATURE
0
1
2
3
4
5
6

Fig. 2d

Fig. 3

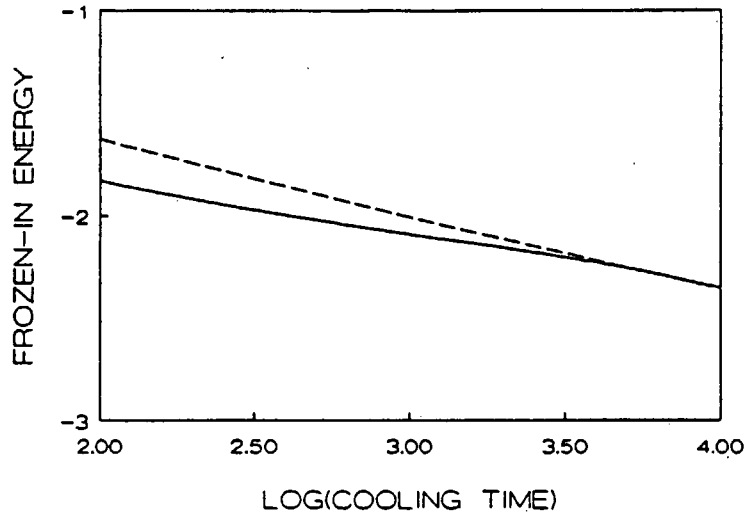

Fig. 3

)4a

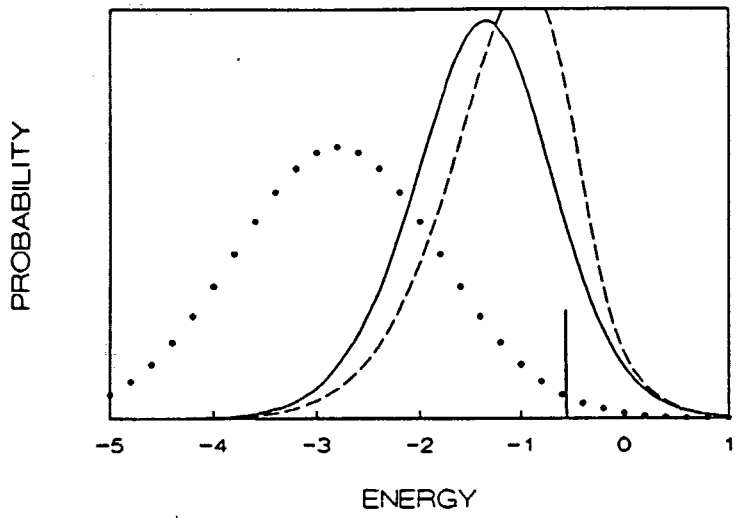

Fig. 4a

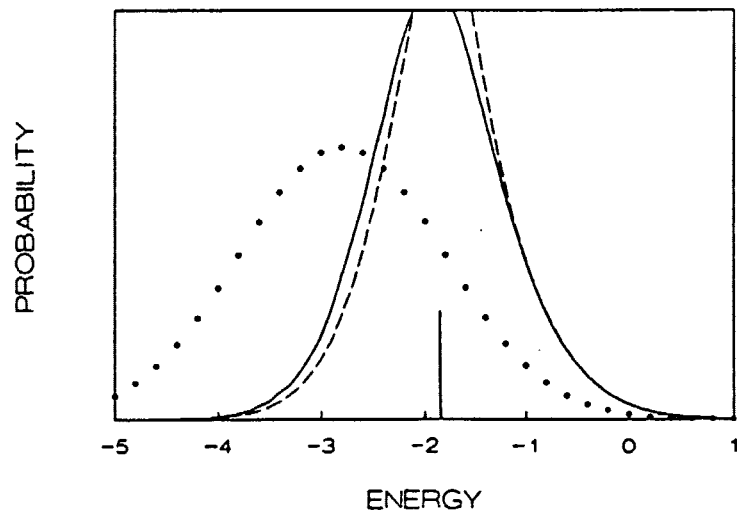

Fig. 4b

ig. 4c

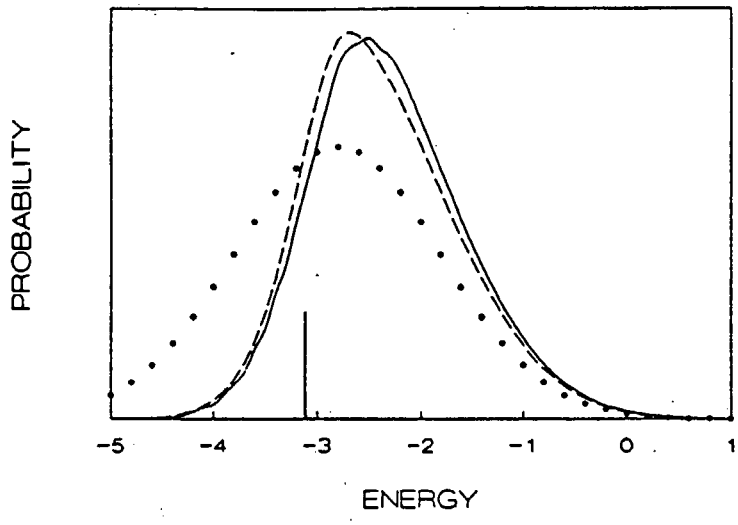

Fig. 4c

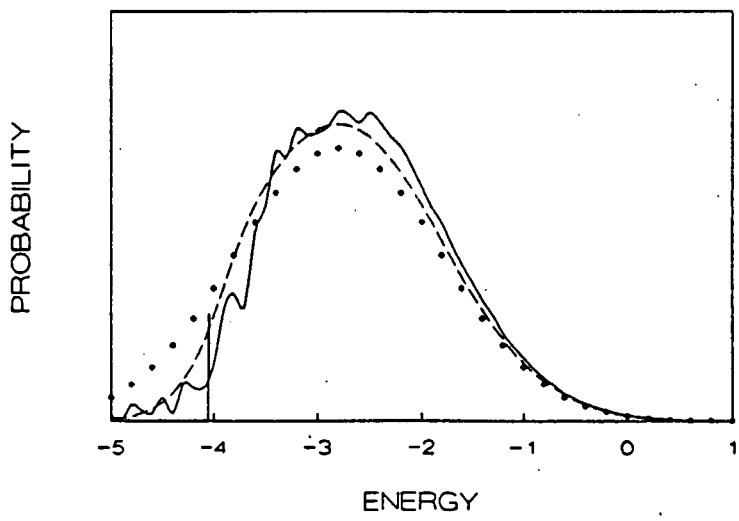

Fig. 4d

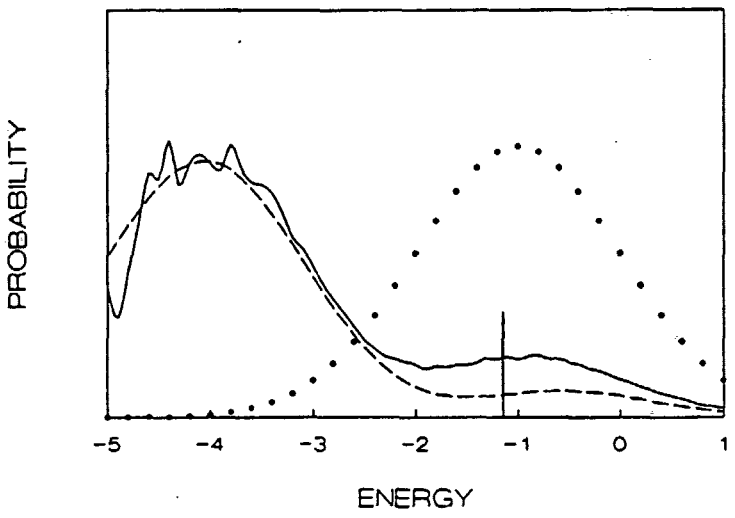

Fig. 5a

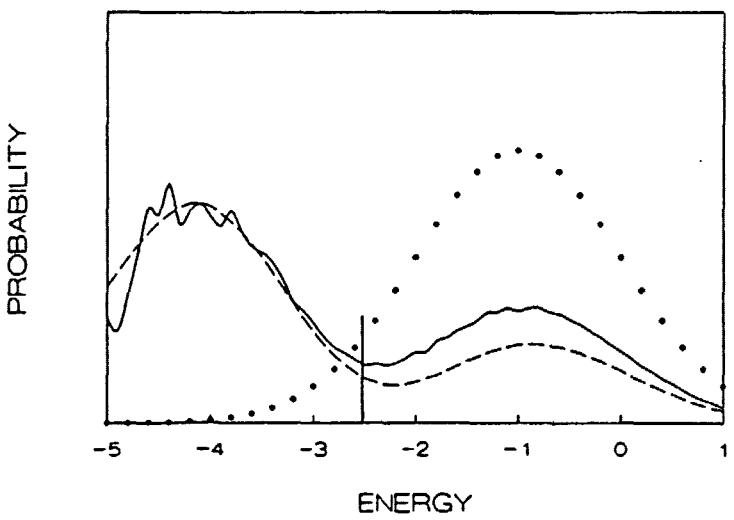

Fig. 5b

g. 5c

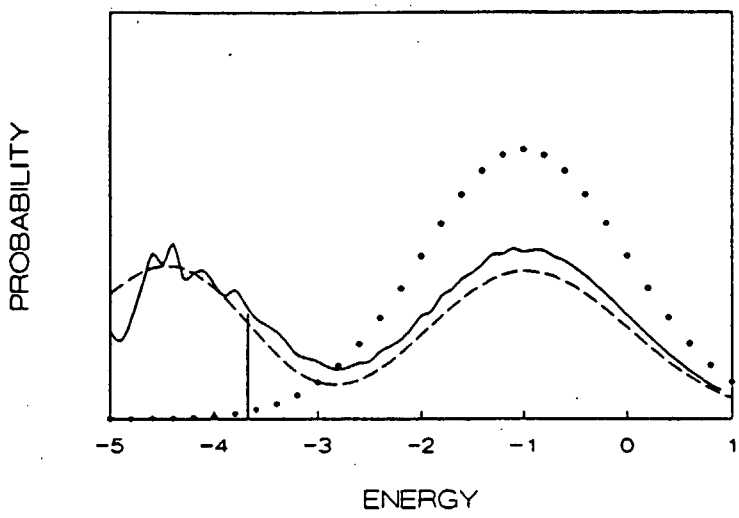

Fig. 5c

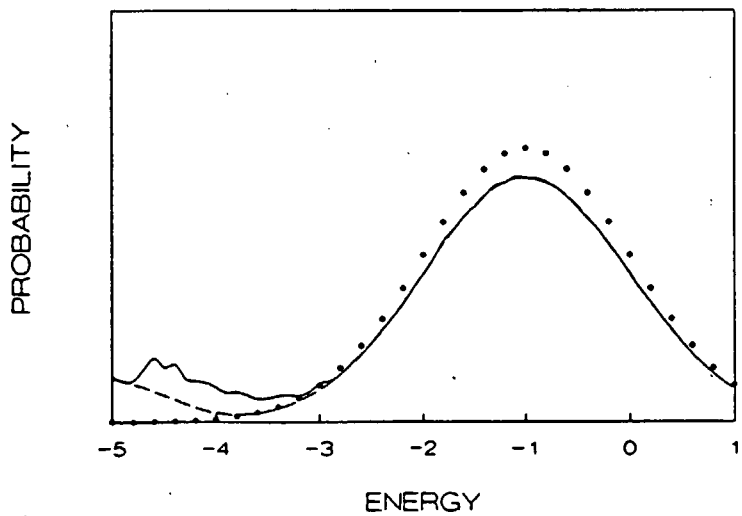

Fig. 5d

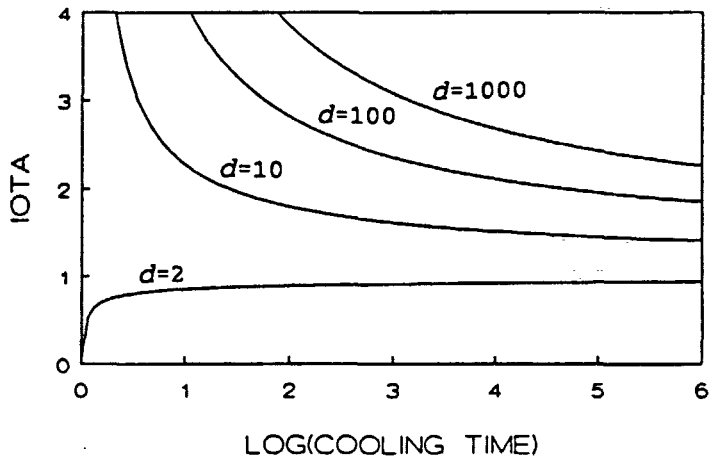

Fig. 6

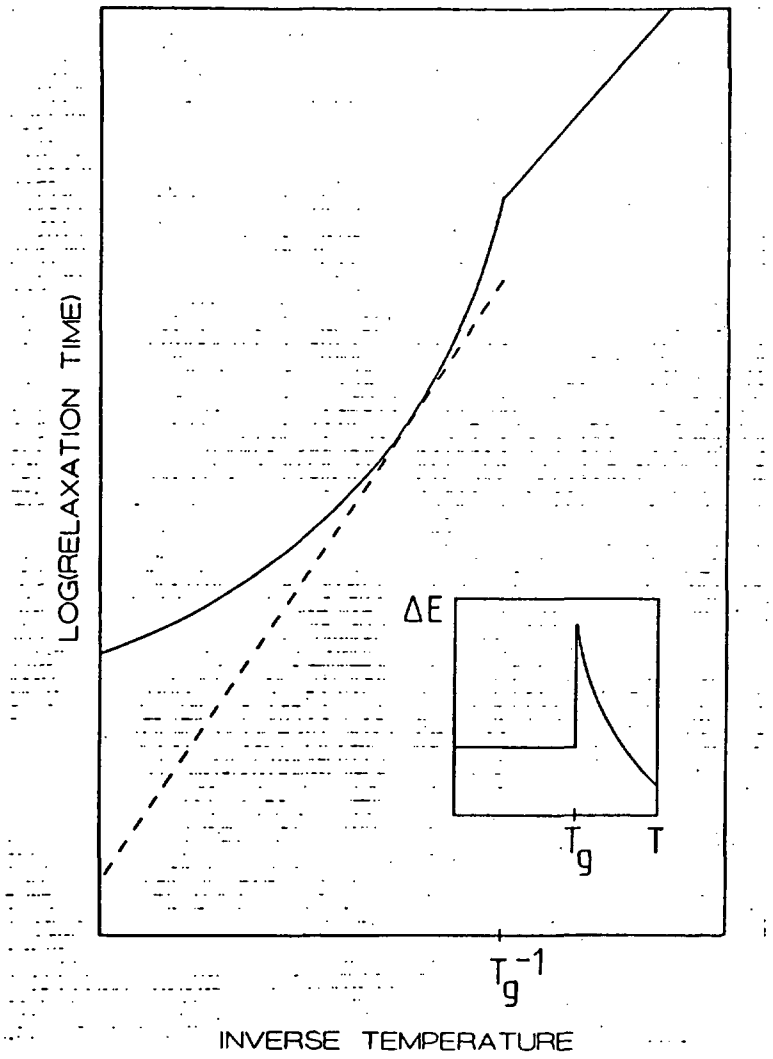
LOG(RELAXATION TIME)
ΔE
T_g
T
T_g^{-1}
INVERSE TEMPERATURE

Fig. 7a

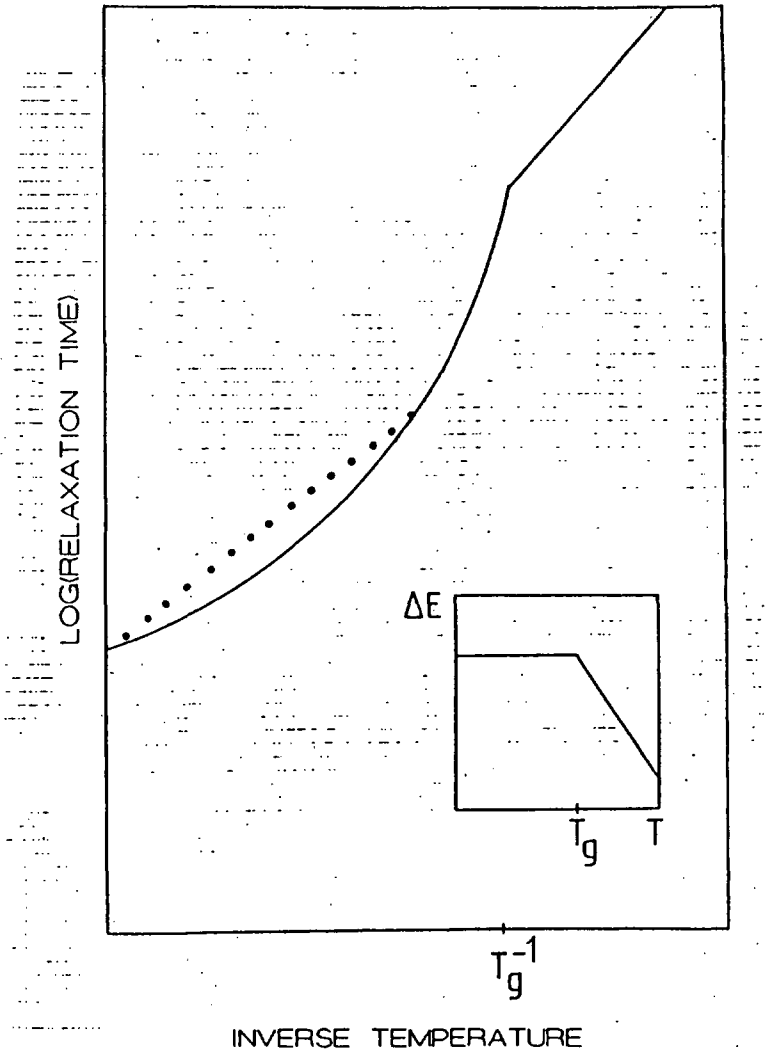
LOG(RELAXATION TIME)
ΔE
T_g
T
T_g^{-1}
INVERSE TEMPERATURE

Fig. 7b

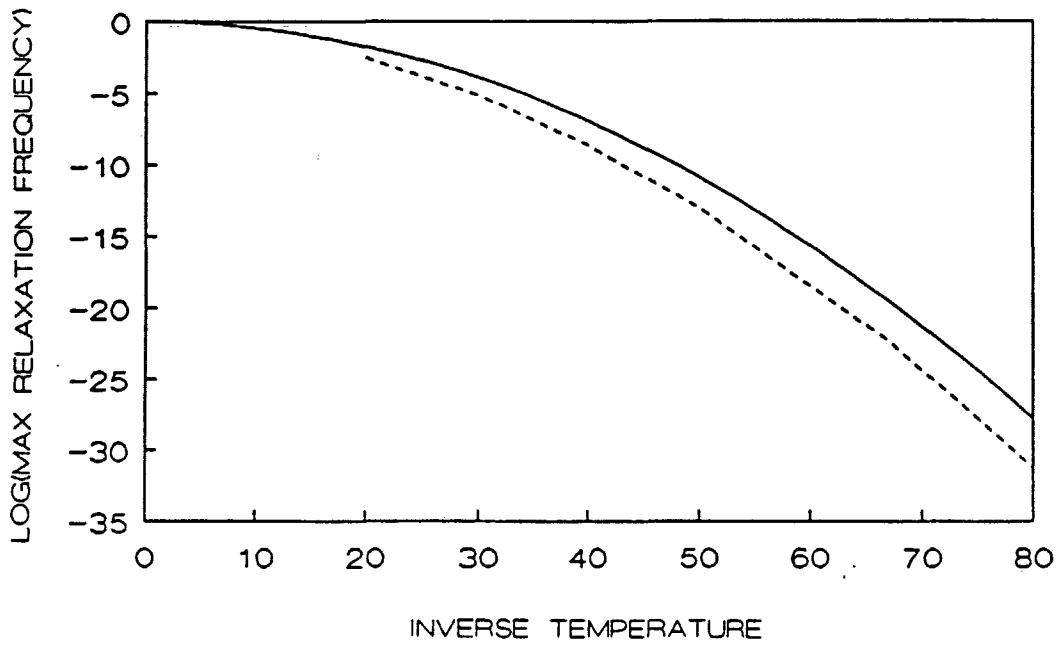
LOG(MAX RELAXATION FREQUENCY)
0
-5
-10
-15
-20
-25
-30
-35
0
10
20
30
40
50
60
70
80
INVERSE TEMPERATURE

Fig. 8

Liste over tidligere udkomne tekster tilsendes gerne. Henvendelse herom kan ske til IMFUFA's sekretariat tlf. 46 75 77 11 lokal 2263

217/92 "Two papers on APPLICATIONS AND MODELLING IN THE MATHEMATICS CURRICULUM"
by: Mogens Niss

218/92 "A Three-Square Theorem"
by: Lars Kadison

219/92 "RUPNOK - stationær strømning i elastiske rør"
af: Anja Boisen, Karen Birkelund, Mette Olufsen
Vejleder: Jesper Larsen

220/92 "Automatisk diagnosticering i digitale kredsløb"
af: Bjørn Christensen, Ole Møller Nielsen
Vejleder: Stig Andur Pedersen

221/92 "A BUNDLE VALUED RADON TRANSFORM, WITH APPLICATIONS TO INVARIANT WAVE EQUATIONS"
by: Thomas P. Branson, Gestur Olafsson and Henrik Schlichtkrull

222/92 On the Representations of some Infinite Dimensional Groups and Algebras Related to Quantum Physics
by: Johnny T. Ottesen

223/92 *THE FUNCTIONAL DETERMINANT*
by: Thomas P. Branson

224/92 *UNIVERSAL AC CONDUCTIVITY OF NON-METALLIC SOLIDS AT LOW TEMPERATURES*
by: Jeppe C. Dyre

225/92 *"HATMODELLEN" Impedansspektroskopi i ultrarent en-krystallinsk silicium*
af: Anja Boisen, Anders Gorm Larsen, Jesper Varmer, Johannes K. Nielsen, Kit R. Hansen, Peter Bøggild og Thomas Hougaard
Vejleder: Petr Viscor

226/92 *"METHODS AND MODELS FOR ESTIMATING THE GLOBAL CIRCULATION OF SELECTED EMISSIONS FROM ENERGY CONVERSION"*
by: Bent Sørensen

227/92 "Computersimulering og fysik"
af: Per M.Hansen, Steffen Holm, Peter Maibom, Mads K. Dall Petersen, Pernille Postgaard, Thomas B.Schrøder, Ivar P. Zeck
Vejleder: Peder Voetmann Christiansen

228/92 "Teknologi og historie"
Fire artikler af:
Mogens Niss, Jens Høyrup, Ib Thiersen, Hans Hedal

229/92 "Masser af information uden betydning"
En diskussion af informationsteorien i Tor Nørretranders' "Mærk Verden" og en skitse til et alternativ basseret på andenordens kybernetik og semiotik.
af: Søren Brier

230/92 "Vinklens tredeling - et klassisk problem"
et matematisk projekt af
Karen Birkelund, Bjørn Christensen
Vejleder: Johnny Ottesen

231A/92 "Elektrondiffusion i silicium - en matematisk model"
af: Jesper Voetmann, Karen Birkelund, Mette Olufsen, Ole Møller Nielsen
Vejledere: Johnny Ottesen, H.B.Hansen

231B/92 "Elektrondiffusion i silicium - en matematisk model" Kildetekster
af: Jesper Voetmann, Karen Birkelund, Mette Olufsen, Ole Møller Nielsen
Vejledere: Johnny Ottesen, H.B.Hansen

232/92 "Undersøgelse om den simultane opdagelse af energiens bevarelse og især om de af Mayer, Colding, Joule og Helmholtz udførte arbejder"
af: L.Arleth, G.I.Dybkjær, M.T.Østergård
Vejleder: Dorthe Posselt

233/92 "The effect of age-dependent host mortality on the dynamics of an endemic disease and
Instability in an SIR-model with age-dependent susceptibility
by: Viggo Andreasen

234/92 "THE FUNCTIONAL DETERMINANT OF A FOUR-DIMENSIONAL BOUNDARY VALUE PROBLEM"
by: Thomas P. Branson and Peter B. Gilkey

235/92 OVERFLADESTRUKTUR OG POREUDVIKLING AF KOKS
- Modul 3 fysik projekt -
af: Thomas Jessen

236a/93 INTRODUKTION TIL KVANTE HALL EFFEKTEN

af: Anja Boisen, Peter Bøggild

Vejleder: Peder Voetmann Christiansen
Erland Brun Hansen

236b/93 STRØMSSAMMENBRUD AF KVANTE HALL EFFEKTEN

af: Anja Boisen, Peter Bøggild

Vejleder: Peder Voetmann Christiansen
Erland Brun Hansen

237/93 The Wedderburn principal theorem and Shukla cohomology

af: Lars Kadison

238/93 SEMIOTIK OG SYSTEMEGENSKABER (2)

Vektorbånd og tensorer

af: Peder Voetmann Christiansen

239/93 Valgsystemer - Modelbygning og analyse

Matematik 2. modul

af: Charlotte Gjerrild, Jane Hansen, Maria Hermannsson, Allan Jørgensen, Ragna Clauson-Kaas, Poul Lützen

Vejleder: Mogens Niss

240/93 Patologiske eksempler.
Om sære matematiske fisks betydning for den matematiske udvikling

af: Claus Dræby, Jørn Skov Hansen, Runa Ulsøe Johansen, Peter Meibom, Johannes Kristoffer Nielsen

Vejleder: Mogens Niss

241/93 FOTOVOLTAISK STATUSNOTAT 1

af: Bent Sørensen

242/93 Brovedligeholdelse - bevar mig vel

Analyse af Vejdirektoratets model for optimering af broreparationer

af: Linda Kyndlev, Kare Fundal, Kamma Tulinius, Ivar Zeck

Vejleder: Jesper Larsen

243/93 TANKEEKSPERIMENTER I FYSIKKEN

Et 1.modul fysikprojekt

af: Karen Birkelund, Stine Sofia Korremann

Vejleder: Dorthe Posselt

244/93 RADONTRANSFORMATIONEN oq dens anvendelse i CT-scanning

Projektrapport

af: Trine Andreasen, Tine Guldager Christiansen, Nina Skov Hansen og Christine Iversen

Vejledere: Gestur Olafsson og Jesper Larsen

245a+b /93 Time-Of-Flight målinger på krystallinske halvledere
Specialerapport

af: Linda Szkotak Jensen og Lise Odgaard Gade

Vejledere: Petr Viscor og Niels Boye Olsen

246/93 HVERDAGSVIDEN OG MATEMATIK - LÆREPROCESSER I SKOLEN

af: Lena Lindenskov, Statens Humanistiske Forskningsråd, RUC, IMFUFA

247/93 UNIVERSAL LOW TEMPERATURE AC CONDUCTIVITY OF MACROSCOPICALLY DISORDERED NON-METALS

by: Jeppe C. Dyre

248/93 DIRAC OPERATORS AND MANIFOLDS WITH BOUNDARY

by: B. Booss-Bavnbek, K.P.Wojciechowski

249/93 Perspectives on Teichmüller and the Jahresbericht Addendum to Schappacher, Scholz, et al.

by: B. Booss-Bavnbek

With comments by W.Abikoff, L.Ahlfors, J.Cerf, P.J.Davis, W.Fuchs, F.P.Gardiner, J.Jost, J.-P.Kahane, R.Lohan, L.Lorch, J.Radkau and T.Söderqvist

250/93 EULER OG BOLZANO - MATEMATISK ANALYSE SET I ET VIDENSKABSTEORETISK PERSPEKTIV

Projektrapport af: Anja Juul, Lone Michelsen, Tomas Højgård Jensen

Vejleder: Stig Andur Pedersen

251/93 Genotypic Proportions in Hybrid Zones

by: Freddy Bugge Christiansen, Viggo Andreasen and Ebbe Thue Poulsen

252/93 MODELLERING AF TILFÆLDIGE FÆNOMENER

Projektrapport af: Birthe Friis, Lisbeth Helmgaar, Kristina Charlotte Jakobsen, Marina Mosbæk Johannessen, Lotte Ludvigsen, Mette Hass Nielsen

253/93 Kuglepakning

Teori og model

af: Lise Arleth, Kåre Fundal, Nils Kruse

Vejleder: Mogens Niss

254/93 Regressionsanalyse

Materiale til et statistikkursus

af: Jørgen Larsen

255/93 TID & BETINGET UAFHÆNGIGHED

af: Peter Harremoës

256/93 Determination of the Frequency Dependent Bulk Modulus of Liquids Using a Piezoelectric Spherical Shell (Preprint)

by: T. Christensen and N.B.Olsen

257/93 Modellering af dispersion i piezoelektriske keramikker

af: Pernille Postgaard, Jannik Rasmussen, Christina Specht, Mikko Østergård

Vejleder: Tage Christensen

258/93 Supplerende kursusmateriale til "Lineære strukturer fra algebra og analyse"

af: Mogens Brun Heefelt

259/93 STUDIES OF AC HOPPING CONDUCTION AT LOW TEMPERATURES

by: Jeppe C. Dyre

260/93 PARTITIONED MANIFOLDS AND INVARIANTS IN DIMENSIONS 2, 3, AND 4

by: B. Booss-Bavnbek, K.P.Wojciechowski

261/93 OPGAVESAMLING
Bredde-kursus i Fysik
Eksamensopgaver fra 1976-93

262/93 Separability and the Jones Polynomial
by: Lars Kadison

263/93 Supplerende kursusmateriale til "Lineære strukturer fra algebra og analyse" II
af: Mogens Brun Heefelt

264/93 FOTOVOLTAISK STATUSNOTAT 2
af: Bent Sørensen

265/94 SPHERICAL FUNCTIONS ON ORDERED SYMMETRIC SPACES
To Sigurdur Helgason on his sixtyfifth birthday
by: Jacques Faraut, Joachim Hilgert and Gestur Olafsson

266/94 Kommensurabilitets-oscillationer i laterale supergitre
Fysikspeciale af: Anja Boisen, Peter Bøggild, Karen Birkelund
Vejledere: Rafael Taboryski, Poul Erik Lindelof, Peder Voetmann Christiansen

267/94 Kom til kort med matematik på Eksperimentarium - Et forslag til en opstilling
af: Charlotte Gjerrild, Jane Hansen
Vejleder: Bernhelm Booss-Bavnbek

268/94 Life is like a sewer ...
Et projekt om modellering af aorta via en model for strømning i kloakrør
af: Anders Marcussen, Anne C. Nilsson, Lone Michelsen, Per M. Hansen
Vejleder: Jesper Larsen

269/94 Dimensionsanalyse en introduktion
metaprojekt, fysik
af: Tine Guldager Christiansen, Ken Andersen, Nikolaj Hermann, Jannik Rasmussen
Vejleder: Jens Højgaard Jensen

270/94 THE IMAGE OF THE ENVELOPING ALGEBRA AND IRREDUCIBILITY OF INDUCED REPRESENTATIONS OF EXPONENTIAL LIE GROUPS
by: Jacob Jacobsen

271/94 Matematikken i Fysikken.
Opdaget eller opfundet
NAT-BAS-projekt
vejleder: Jens Højgaard Jensen

272/94 Tradition og fornyelse
Det praktiske elevarbejde i gymnasiets fysikundervisning, 1907-1988
af: Kristian Hoppe og Jeppe Guldager
Vejledning: Karin Beyer og Nils Hybel

273/94 Model for kort- og mellemdistanceløb
Verifikation af model
af: Lise Fabricius Christensen, Helle Pilemann, Bettina Sørensen
Vejleder: Mette Olufsen

274/94 MODEL 10 - en matematisk model af intravenøse anæstetikas farmakokinetik
3. modul matematik, forår 1994
af: Trine Andreasen, Bjørn Christensen, Christine Green, Anja Skjoldborg Hansen. Lisbeth Helmgaard
Vejledere: Viggo Andreasen & Jesper Larsen

275/94 Perspectives on Teichmüller and the Jahresbericht
2nd Edition
by: Bernhelm Booss-Bavnbek

276/94 Dispersionsmodellering
Projektrapport 1. modul
af: Gitte Andersen, Rehannah Borup, Lisbeth Friis, Per Gregersen, Kristina Vejrø
Vejleder: Bernhelm Booss-Bavnbek

277/94 PROJEKTARBEJDSPÆDAGOGIK - Om tre tolkninger af problemorienteret projektarbejde
af: Claus Flensted Behrens, Frederik Voetmann Christiansen, Jørn Skov Hansen, Thomas Thingstrup
Vejleder: Jens Højgaard Jensen

278/94 The Models Underlying the Anaesthesia Simulator Sophus
by: Mette Olufsen(Math-Tech), Finn Nielsen (RISØ National Laboratory), Per Føge Jensen (Herlev University Hospital), Stig Andur Pedersen (Roskilde University)

279/94 Description of a method of measuring the shear modulus of supercooled liquids and a comparison of their thermal and mechanical response functions.
af: Tage Christensen

280/94 A Course in Projective Geometry
by Lars Kadison and Matthias T. Kromann

281/94 Modellering af Det Cardiovaskulære System med Neural Pulskontrol
Projektrapport udarbejdet af:
Stefan Frello, Runa Ulsøe Johansen, Michael Poul Curt Hansen, Klaus Dahl Jensen
Vejleder: Viggo Andreasen